Thesis Report

Deep Learning and Machine Learning Approaches for Non-Contact Surface Roughness Prediction from Scanning Electron Microscope (SEM) Images

Submitted By

Maria Akter Luthfa

Roll : BFH2011034F

Session:2019-2020

Year-(iv),Term-(ii)

Department of Information & Communication Engineering , Noakhali Science And Technology University

Supervised By

Prof. Dr. Md. Ashikur Rahman Khan

Chairman

Department of Information & Communication Engineering , Noakhali Science And Technology University

Date of Submission: 14 August 2025

STUDENT’S DECLARATION

This thesis is submitted to the Department of Information and Communication Engineering of Noakhali Science & Technology University in partial fulfillment of the requirements for the award of the Bachelor of Science (B.Sc.) Engineering in Information and Communication Engineering (ICE). So, I hereby declare that this report has not been submitted elsewhere for the requirement of any kind of degree, diploma, or publication.

Maria Akter Luthfa

Roll : BFH2011034F
Session:2019-2020
Year-(iv),Term-(ii)
Department of Information
& Communication
Engineering, Noakhali
Science And Technology
University

ACCEPTANCE

I hereby declare that I have checked this thesis and, in my opinion, this thesis is adequate in terms of scope and quality for the award of the degree of Bachelor of Science degree in Information & Communication Engineering.

____

Prof. Dr. Md. Ashikur Rahman Khan

Chairman,

Department of Information & Communication Engineering ,
Noakhali Science And Technology University

ACKNOWLEDGEMENT

I am grateful and would like to express my sincere gratitude to my supervisor Professor Dr. Md. Ashikur Rahman Khan for his germinal ideas, invaluable guidance, continuous encouragement and constant support in making this research possible. He has always impressed me with his outstanding professional conduct, his strong conviction for science, and his belief that a B.Sc. program is only a start of a life-long learning experience. I appreciate his consistent support from the first day I applied to graduate program to these concluding moments. I am truly grateful for his progressive vision about my training in science, his tolerance of my native mistakes, and his commitment to my future carrier.

My sincere thanks to all my classmates and members of the staff of the Information and Communication Engineering Department, NSTU, who helped me in many ways. Last but not the least, I would like to thank my parents for encouraging me and standing with me throughout my life.

ABSTRACT

Surface roughness is crucial to the quality, functionality, and durability of manufactured parts. Nonetheless, there is a problem that conventional methods of contact measurements are costly, time-consuming, and ineffective in analyzing complicated surface geometry. To address these constraints, this work proposes deep and traditional machine learning models to specifically predict surface roughness using Scanning Electron Microscope (SEM) images, eliminating the need for physical probing or handcrafted surface analysis. Titanium alloys as a target material were chosen because of the wide range of essential applications, and SEM images were obtained at various magnification levels to capture the broad range of patterns on their surface. A custom design Convolutional Neural Network (CNN) was constructed and trained to perform regression tasks, and two pre-trained deep learning models, ResNet50 and VGG16, were also used. Simultaneously, the images were used to extract the handcrafted features, which were in turn trained by the conventional machine learning models, such as Support Vector Regression (SVR), Random Forest, and Linear Regression. The findings showed that deep learning models mostly performed better, especially VGG16, than the traditional models by providing higher accuracy and R^2 values above 0.95 in the majority of cases. The developed approach has excellent prospects for application in the real world to high-precision industries, including aerospace, biomedical, and electronic manufacturing sectors, allowing for improved performance control and process optimization speed.

Keywords: Surface Roughness; Surface Roughness Prediction; Scanning Electron Microscope; Convolutional Neural Network; Support Vector Regression; Random Forest; Linear Regression.

Table Of Contents

Content

LIST OF FIGURES

LIST OF TABLES

CHAPTER 1

INTRODUCTION

1.1 INTRODUCTION

The introduction of this paper is covered in this chapter. The thesis study focuses on predicting the surface roughness of machined surfaces from SEM images by using Deep and Machine Learning models. This chapter describes surface roughness and its measurement techniques in the background section, followed by a problem statement in Section 1.3, research objectives in Section 1.4, and a definition of the scope of this study in Section 1.5.

1.2 BACKGROUND

Surface roughness (SR) refers to the texture of the surface and can be defined as the slight, fine irregularities or deviations found on an ideal smooth surface. One of the most vital factors of numerous industrial operations is the roughness of surfaces because this may influence the quality, merit, and utility of the produced products. The implication of this discovery is very vital in many disciplines[1].

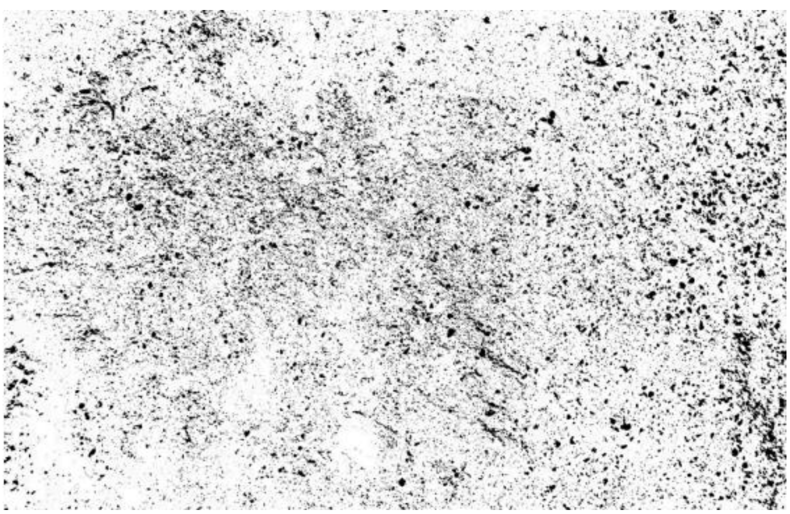

Figure 1.1: Surface image [1]

Surface roughness is generated for the imperfections and irregularities that are formed on the surface material during machining (cutting tools, vibration), manufacturing (casting), or processing [2]. It is generated right at the topmost layer of a material during machining, forming, or processing [3].

SR is essential to quality control and can only be accurately measured. SR can be measured in many ways. The principle will mainly be split into contact and non-contact. We would like to measure the SR using images by Artificial Intelligence (AI). In another aspect, measuring the characteristics of a machined surface can be executed with SEM. Still, it is not possible to get the value of roughness directly without changing hardware, so we can predict the roughness using AI models and can install the model on the SEM machine to get the measurement of SR directly.

Surface roughness or surface finishing is significant in nanotechnology to ascertain how an object uses its environment [4]. This is necessary to address the needs of the existing and newer applications, wherein better features of the surface are vital to ensure better performance and functionality. Then, under mechanical engineering, the Surface roughness affects friction, wear, and lubrication of parts such as bearings and seals. Surface roughness optimization during machining of parts increases their function and life span [5]. It has been established that the roughness can determine the ability of cells to adhere to the material in cases of biomedical engineering [6]. Controlled roughness can affect the integration of a biomedical implant, such as a prosthesis or bone replacement, with the surrounding tissues. It is also able to enhance cell adhesion, differentiation, and growth, eventually contributing to successful implants. Also, the significance of surface roughness lies in one of the most crucial factors in the aerospace industry, which entails guaranteeing the maximum performance, survivability, and safety of both the air and spacecraft. Good measurements of SR are needed to verify strict requirements on the surfaces of aircraft, which are used to improve aerodynamic efficiency and promote security. Besides this, SR measurements are vital to the structural durability of aerospace materials, because cracks and other defects on the surfaces, even microscopic ones, can become disastrous in the long run [7].In addition to this, in the electronics sector, the SR of materials formed of semiconductors also influences the electrical resistance, electron mobility, and heat generation. SR permits better conductivity and effective heat convection, which is vital to the functionality and stability of electronic components, such as microchips, transistors, and integrated circuits. In addition to all this, surface roughness measurement is also used in orthopedics to study the interaction between implants and bones [8]. Likewise, surface roughness in ophthalmology is determined to learn how contact lenses interact with the eye.

Besides surface roughness, surface characteristics are also important in determining the performance and functionality of a material. Roughness, waviness, and lay are part of surface texture and affect friction and contact. Surface energy affects adhesion and coating, and hardness affects wear resistance. The corrosion and biocompatibility are influenced by surface chemistry. In combination, these characteristics make a material perform, and they should all be considered when evaluating surfaces [4].

1.3 PROBLEM STATEMENT

Measurement of SR enables the metrologists to test the roughness of a piece of surface for quality control or any other intentions [1]. Consequently, it is rather vital to measure the surface roughness to control the quality or any other objective, since it is a significant factor that might hinder the fabrication and durability of the piece. At extreme roughness, the friction is higher, and the wear rate increases, leading to premature failure in mechanical components. Conversely, unnaturally smooth surfaces might not easily maintain sufficient lubrication due to the occurrence of friction and wear. Research indicates that surface texture and roughness, and their effects on the surface, can have a profound influence on the capacity of lubricant to bear load [9].

Surface roughness is measured in several ways. These are the various methods, which can be divided into two sections: contact methods and non-contact methods.

Contact techniques imply the physical correlation between the measuring device and the testing surface. Traditional statistical techniques of surface roughness measurements may prove rigid, time wasting, costly, and limited in precision. They experience problems in explaining complex parameter interactions with process parameters and understanding the mechanisms. The conventional intrusive methods may deform soft materials, give inaccurate results, and limit the operation to offline, resulting in inappropriateness in high-speed, real-time production processes. They have also not been used to measure three-dimensional surface detail or fine-scale variations, and they are very operator-dependent, leading to subjectiveness and possible error. The issues above reveal the necessity of non-contact, real-time, automated, and innovative SR measurement technologies to produce accurate, repeatable, and effective surface quality measurements in contemporary manufacturing.

Non-contact methods that analyze the surface without contact rely on visual or electromagnetic principles to gauge the surface roughness. The methods are most appropriate for fragile, delicate, or intricate surfaces. As a case study, the dark/bright ratio (DBR) method is an innovative optical method of measuring surface roughness on a moving surface. The technique relies on speckle patterns and scattering to measure roughness based on the proportion of dark and light spots in the speckle image. The experimental evidence of measurement reliability across alternative DBR approaches is based on the findings that the method can and does give measurements as good as the conventional stylus methods, with differences of less than 5 percent in different speeds (up to 0.017 m/s). It has been determined that the DBR process is relatively easy, accurate, and can be used to measure during the process, thus demonstrating its application in industries [10].

There are a few approaches that have been used to calculate and forecast SR over the years, which include Taguchi-based regression models [11,12], statistical regression models [13], computational approaches (such as the Finite Element Method and Discrete Element Method) [14], and Machine Learning approaches [15]. Although they are primarily used, old methods of measurement and prediction of SR have numerous limitations that curtail their applicability in contemporary industrial settings.

The emergence of Artificial Intelligence technology, such as Machine Learning and Deep Learning (DL), has transformed the way we solve the same. AI methods provide opportunities for more accurate and flexible surface roughness predictions [16]. Further improvement on Surface Roughness prediction can be done via vibration signal analysis and presented as Deep Learning Neural Networks. The process in view would be to use the vibration signal to effectively say that it is a non-contact and real-time measurement of what surface roughness will appear to be, and this is making up one of the shortcomings of the traditional methods of measurement, being a contact-based application. However, the quality of the data on the vibration signal significantly influences the accuracy of deep learning models in terms of quality, quantity, and variety. The limited or noisy datasets may decrease the ability of the model to capture meaningful patterns [17]. A method called machine vision to find the roughness of surfaces is presented that uses the image processing method [18]. However, the lighting condition, shadows, or reflections during image acquisition may introduce inconsistency in the accuracy of the method. Therefore, we require a method that is reliable and non-contact to carry out surface measurements. We would like to measure the SR with images through an Artificial Intelligence model that can be installed on the SEM machine in the future to derive the value of SR measured directly by SEM.

1.4 OBJECTIVES

The primary aim of the work is to quantify the roughness level of a machined surface using image data obtained with the SEM and to utilize AI models in this regard. SR prediction is often determined by contact methods, which waste plenty of time, cost a lot of money, and, additionally, deform fragile materials, which provides inaccurate results. The non-contact method to measure roughness is the foundation of our research idea. The installation of the best AI model into the SEM machine can help one get the SR value directly in the future. The following are some of the objectives:

1. To predict the Surface roughness value of a machined surface using images by Deep and Machine Learning models.
2. To shorten the time, cost, and complexity associated with surface roughness measurement significantly.
3. To study the effect of various magnification values on the accuracy of predicting surface roughness.
4. To investigate how well trained models generalize when tested on unseen images.
5. To compare Deep Learning (CNNs) with traditional Machine Learning models.

1.5 SCOPE OF THE RESEARCH

The amenities of this research involve the following factors: data acquisition, application areas, and tools/software. To train or test the CNN model and moderate approaches, the SEM images of titanium alloy materials are used. This can be concentrated on industries like aerospace, automotive, electronics, and research and development, where the quality of surfaces influences functionality and reliability. The tools that will be utilized in the development of the model will include- TensorFlow, Google Colab or Kaggle, openCV or Matplotlib, etc.

Hardware Need: Computer (intel core i3, windows 10 OS)

Software Requirement: Google Colab.

Computer Programming Language: Python.

CHAPTER 2

LITERATURE REVIEW

2.1 INTRODUCTION

This chapter reviews prior research efforts on surface roughness measurement using various techniques. Section 2.2 describes the procedures employed in SR measurement and highlights their relevance. Then, a summary of previous works is shown in a tabular format. Then, in the next section, the limitations of previous research are described.

2.2 METHODS FOR SURFACE ROUGHNESS MEASUREMENT

For measuring surface roughness, there have been various techniques applied to date. These various methods are mainly categorized into two parts – contact and non-contact methods. Contact methods involve physical interaction between the measuring instrument and the surface being tested, and non-contact methods do not require physical interaction, which is why these methods are particularly suitable for delicate, soft, or complex surfaces.

2.2.1 Conventional Methods for Surface Roughness Measurement

The initial studies in surface roughness prediction were primarily based on conventional methods rather than machine-learning methods. The contact method works based on dragging a diamond-tipped stylus on the surface, and the tip size is created to scar the finite part of the surface geometry. The stylus is hooked onto an arm, which in turn is connected with a transducer as shown in Fig. 2 .1. Differences in the surface height will bring the stylus into motion, leading to an alteration in the signal that is recorded and enhanced by the transducer and other associated electronics. The inductance principle of transducer is the most widely used one, providing a large ratio of range to resolution, and a very sturdy construction [19]. When reviewed in detail, these methods were further classified into three main categories, namely: machining theory, experimental analysis, and design of experiments [20]. As another illustration, Sudianto, A. et al. considered a comparative study of regression methods to predict SR, which exploited more diverse offcut parameters, namely, spindle speed, offcut velocity, feed rate, depth of cut (DOC), length of cut (LOC), helix angle, and nose radius [21]. These methods, with the help of a stylus or probe, physically trace the surface, and the variations in height at each point on the surface are measured. Some contact methods are the stylus profilometry, atomic force microscopy (AFM), and mechanical methods, such as surface roughness comparator plates.

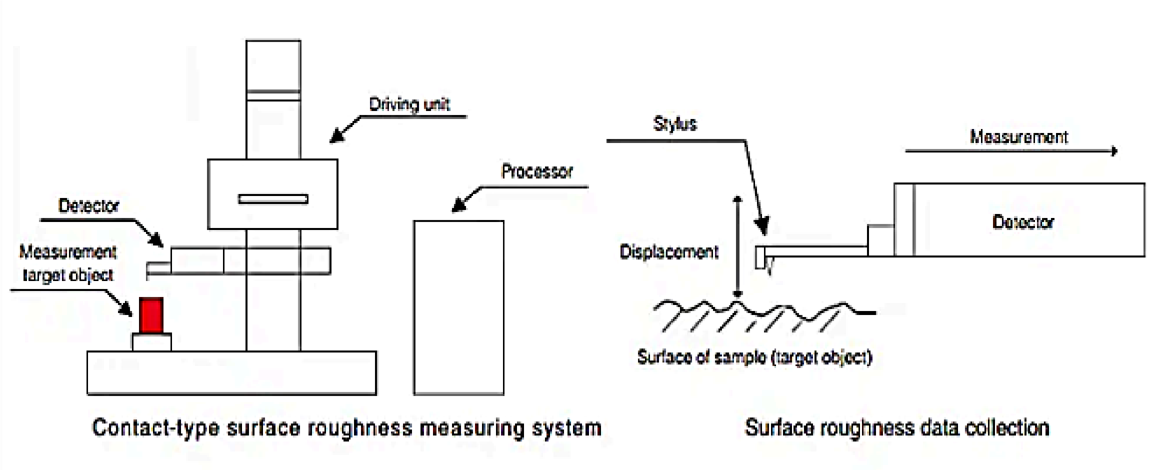

Figure 2.1: Stylus-based SR measurement [1]

2.2.2 Non-Contact Measurement Systems

G. Samtas (2014) created a non-contact system of predicting surface roughness based on the use of two dissimilar materials. These materials were turned on a CNC (Computer Numerical Control) milling machine using some cutting parameters that affected the surface roughness. The characterizations on the resulting surface images were used to develop artificial neural networks to predict roughness accurately [22]. C. Bradley proposed an automated device, which is a combination of a non-contact optical surface roughness probe and a CNC coordinate measuring machine (CMM). The system was meant to acquire the surface roughness (SR) on non-planar and complex-shaped surfaces, such as the turbine blade, with better precision and flexibility to the complex geometries [23]. Dark/bright ratio (DBR) is an innovative optical procedure to record the SR in non-contact and real-time measurements of moving surfaces [24]. Cheng et al. also highlight the power of using Gaussian Process Regression (GPR) to predict SR, as it outperforms other models [25]. GPR was especially appropriate for smaller and medium-sized data, including large numbers of variables.

Figure 2.2**:** Non-contact method [1]

2.2.3 Genetic Algorithms and Image-Based Approaches

M. Rajaram Narayanan et al. (2007) have come up with a genetic algorithm-based EHW (Evolvable Hardware) chip to test the surface roughness of the parts that need to be manufactured using milling [26]. The scheme was based on processing surface images to reduce noise and improve the accuracy of the measurement. As reported in the experiments, the method proposed here was conducted reliably in quantitatively determining the roughness of machined surfaces. In addition, regression analysis showed that improvements in image quality with the EHW system improved the correlation compared to the case when there was no enhancement. This study also identified the possibility of using the artificial neural network in future studies to predict the surface roughness by feeding image properties as data. Another study that assessed the impacts of different machining tool factors on SR in carbon fiber composite plates of high strength under the dry-end milling effect deployed a hybrid method, consisting of ANN and Genetic Algorithm (GA) that showed an outstanding performance in predicting the data [27].

2.2.4 Machine Learning Techniques and Deep Learning

Nicholas E. Sizemore (2019) draws attention to the predictive capabilities of Artificial Neural Networks (ANN) and traditional Machine Learning-based tools, Random Forest, Decision Trees, AdaBoost, and Support Vector Machines, in predicting the surface roughness of diamond turning of germanium (Ge) and copper (Cu). Although the finite element analysis (FEA) models ductile materials such as copper well, it fails to do so under brittle materials such as germanium. The paper evidences that ML and ANN can eliminate these deficiencies and can enhance the accuracy of predictions on each type of material [28]. Wenhe Zhang (2021) forecasted the surface roughness on Al6061 using the Machine Learning models involving linear regression, random forest, decision tree, and neural networks. Neural networks delivered the highest score with an MAE of 0.00279 and an RMSE of 0.00770. Posing the task as a regression problem, Zhang studied the relationship between the features using a dataset of 48 records that included the information about the rotational speed, feed rate, cutting depth, surface roughness, and applied the results to the model [29]. Surface roughness output of machined aluminum alloys using WEDM can be predicted with machine learning, enabling fast and accurate predictions without requiring complicated experiments, as demonstrated by Mustafa Ulas et al. (2020). They put together Extreme Learning Machine (ELM) and Support Vector Regression, and the non-iterative training of ELM was much faster than the iterative training of SVR. The roughness of the surface was between 2.490 and 3.177, and the models are helpful in WEDM-based manufacturing [30]. The second research presented the effective creation of an optical image-surface roughness dataset and suggested the SSEResNet regression model that predicts the surface roughness by combining features. Among all those CNN backbone networks, SSEResNet appeared to work the best in obtaining detailed information on optical images in terms of predictive performance [31].

2.2.5 Applications of Convolutional Neural Networks

Among the possible methods of image processing, we can find the Convolutional Neural Networks, which are the most promising and effective when dealing with deep learning for surface classification. Caggiano et al. [32] have designed a laser polishing procedure using a CNN, where polishing parameters were chosen based on the surface situations that were anticipated using the CNN model. On the same note, Zhang et al. [33] characterized how CNNs can be used to predict and type out surface images of additive manufacturing (AM) procedures. Weimer et al. [34] have developed a deep CNN that is trained to detect and classify defects that appear on machined surfaces automatically. In this case, CNN will systematically draw relevant characteristics of the training dataset to effectively forecast the defects on the surface with minimal human intervention [35]. In another work, a hybrid model was introduced based on a combination of deep learning and theoretical modeling to achieve high accuracy of prediction and understand the effects that grain boundaries and processing parameters have on the SR of diamond-turned polycrystalline materials [36].

2.2.6 Surface Characteristics Determination Using SEM

A Scanning Electron Microscope is an advanced imaging device that is used to examine the surface structure and composition of materials at very high magnifications, often at the nanoscale. In a study, the SEM analysis of titanium alloy Ti-5Al-2.5Sn machined with copper, copper-tungsten, and graphite electrodes examined the microstructure of the machined surface. The machined surface presented the least crater size, the least cracking, and the most significant amount of globules. These characteristics show a more consistent surface finish, and are smoother, and therefore copper is the best and ideal electrode where high surface quality is needed [37].

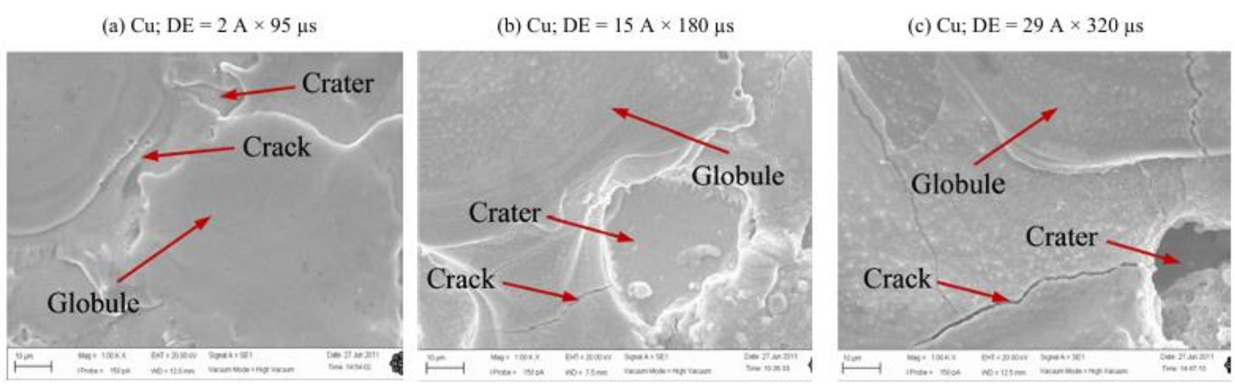

Figure 2.3: Surface characteristics [37]

In a study, surface roughness was measured using a standard Scanning Electron Microscope by making specific hardware modifications. Backscattered Electron Signal (BES) output was used to analyze surface slope and roughness [38].

Table 2.1: Review of similar studies on Surface Roughness measurement

Author	Title	Used Material	Methods	Findings	Limitation
C. Bradley	"Automated Surface Roughness Measurement "	Curved surfaces (e.g., turbine blades)	Optical SR sensor integrated with a CNC coordinate measuring machine	Achieved high precision and adaptability for complex geometries, enabling improved surface measurement.	Costly, non-portable and unsuitable for real-time monitoring
Cheng et al. (2020)	"Prediction of surface residual stress in end milling with Gaussian process regression"	Yield Strength and Tensile Strength Materials	Gaussian Process Regression	Superior R-squared values compared to other models, suitable for datasets with numerous independent variables.	High computational complexity, and may struggle with a noisy dataset
Caggiano et al.	"Automated laser polishing for surface finish enhancement of additive manufactured components for the automotive industry"	Laser-polished surfaces	CNN	CNN predicted surface conditions effectively, enabling parameter optimization for laser polishing	Its effectiveness depends on a large dataset and may not perform well on different materials without retaining.
Zhang et al.	"Surface Roughness Prediction with Machine Learning"	Additively manufactured surfaces	CNN	Successfully predicted and classified surface images generated through additive	Depends on a large dataset and may not perform well on different materials

				manufacturing processes.	
Weimer et al.	“Design of deep convolutional neural network architectures for automated feature extraction in industrial inspection”	Machined surfaces	Deep Convolutional Neural Network	Automatic detection and classification of defects with minimal human intervention, extracting relevant features systematically.	The model needs extensive training data and computational resources.
M. Rajaram Narayanan et al.	"Online surface roughness measurement using image processing and machine vision"	Machined Components	Preprocessed surface images with ANN	Improved correlation of regression analysis by enhancing image quality, indicating reliable surface roughness evaluation.	Accuracy drops with varying lights and may not generalize well to different materials.
Wenhe Zhang(2021)	“Surface Roughness Prediction with Machine Learning”	Al6061 aluminum alloy	Linear Regression, Decision Tree, Random Forest, Neural Network	MAE and RMSE values are 0.00279, 0.00770	The study does not test how well the models handle varied real-world data

Nicholas E. Sizemore,(2019)	“Application of machine learning to the prediction of surface roughness in diamond machining”	Single-crystal Ge and Cu	ANN, SVM, AdaBoost, Decision Tree, Random Forest,	ANN model showed the best overall fit concerning RMSE Ge and Cu	Limited dataset size and lack of real-time testing
Mustafa Ulas et al. (2020)	“Surface roughness prediction of machined aluminum alloy with wire electrical discharge machining by different machine learning algorithms”	Al7075 aluminum alloy	ELM, W-ELM, SVR, Q-SVR	Lowest surface roughness value 2.490	The models are tested only on Al7075, limiting their use for other materials.

2.3 RESEARCH GAP

While significant advancements have been made in surface roughness prediction using traditional methods and machine learning techniques, critical research gaps remain, particularly in leveraging Scanning Electron Microscope images with Convolutional Neural Networks. Current studies often rely on limited datasets with inconsistent magnification levels and variable image quality, which hinder the development of generalizable models. Additionally, the lack of standardized SEM imaging protocols further complicates the reproducibility and scalability of these approaches.

Existing methods predominantly focus on materials such as aluminum and steel, leaving titanium alloys and other advanced materials underexplored. Furthermore, while SEM provides detailed surface texture analysis, its potential for directly predicting SR using CNNs remains largely untapped. A comprehensive approach that integrates SEM images with machining parameters or material properties is also absent, limiting the understanding of how surface features influence roughness outcomes. The research gap of directly using SEM suggests that there is a need for further research to develop and optimize CNN models designed explicitly for SR prediction from SEM images, which could offer superior accuracy and insights into microstructural surface characteristics compared to existing methods. Therefore, it is possible to predict the surface roughness directly from SEM by CNN.

2.4 SUMMARY

The prediction of surface roughness plays a critical role in ensuring the quality control of manufactured components. While sensor-based measurement techniques offer high accuracy, they are often expensive, time-consuming, and unsuitable for real-time industrial use. Deep learning approaches—particularly Convolutional Neural Networks (CNNs)—have shown promising results in predicting surface roughness from image data. However, these models generally require large datasets and significant computational resources. A key limitation of many existing models is their poor ability to generalize across varying conditions such as different materials, lighting environments, and machining parameters. These challenges hinder their adoption in practical, real-time manufacturing settings.

To address these limitations, this study contributes in several essential ways. It predicts surface roughness values directly from scanning electron microscope (SEM) images of machined surfaces using both deep learning and traditional machine learning models. The aim is to significantly reduce the time, cost, and complexity typically involved in surface roughness measurement. Additionally, the study investigates the influence of different magnification levels on prediction accuracy, providing insight into the optimal imaging conditions for reliable results. It also evaluates how well the trained models generalize when tested on unseen images, a critical factor for real-world deployment. Finally, by comparing the performance of CNN-based models with conventional machine learning algorithms, this work offers a comprehensive understanding of their relative strengths and limitations. Overall, the goal is to develop more efficient, generalizable, and real-time-capable solutions for automated quality control in manufacturing.

CHAPTER 3

METHODOLOGY

3.1 INTRODUCTION

This chapter narrates the implementation of the CNN regression model and moderate method with SVR, Random Forest, and Linear Regression for predicting surface roughness from images. Section 3.2 shows the strategy of the work frame. Section 3.3 illustrates the data collection and data preprocessing. In the next section, the development of both models and the performance evaluation are described.

3.2 STRATEGY OF WORK FRAME

The given study is organized in the following forms: data collection, data processing, development of AI models, training and testing of the AI models, and performance assessment. The sections are tackled in a systematic manner, placing them into small, manageable steps. Fig. 3.1 can show the general steps involved in predicting surface roughness and helps explain how the research is carried out.

Figure 3.1: Workflow of methodology

3.3 DATA COLLECTION

The first stage is data acquisition of images. In this study, the SEM has been used to obtain images of titanium alloy material that has been machined in an Electrical discharge machine, based on its surface characteristics. In Electrical Discharge Machining, titanium alloys are cut using electrical sparks, leaving a rough surface. The measurement of surface roughness follows machining in a non-contact or contact manner. A Scanning Electron Microscope is thereafter utilized to examine the machined surface, and on that surface, one gets an image. All these surface images are captured from the paper [39-48], and they are taken with the permission of the authorities. Images for 150x magnifications are as follows:

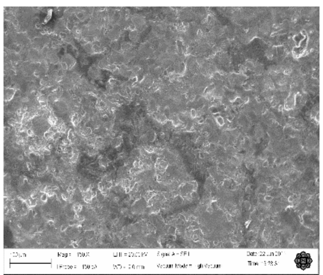

Sl N. 1

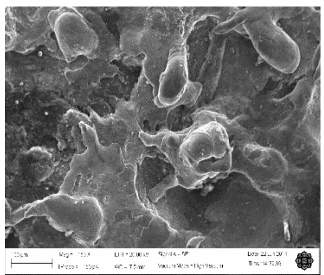

Sl N. 2

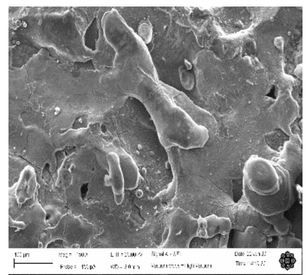

Sl N. 3

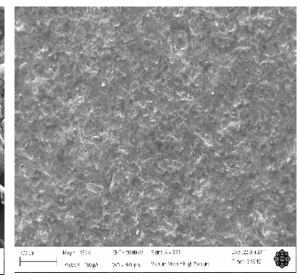

Sl N. 4

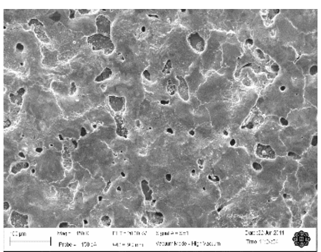

Sl N. 5

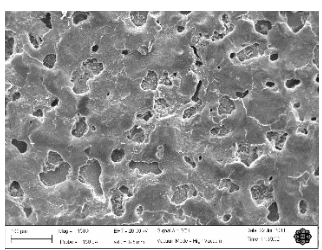

Sl N. 6

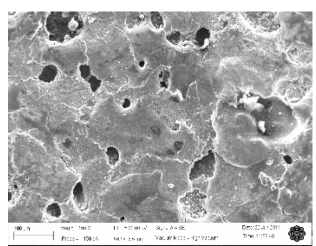

Sl N. 7

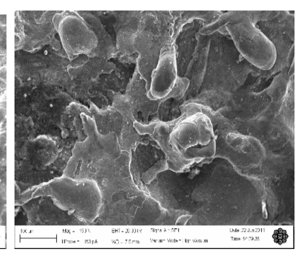

Sl N. 8

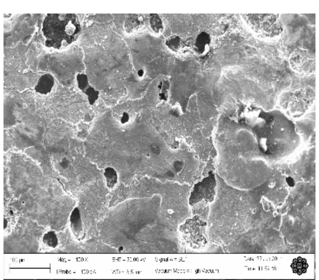

Sl N. 9

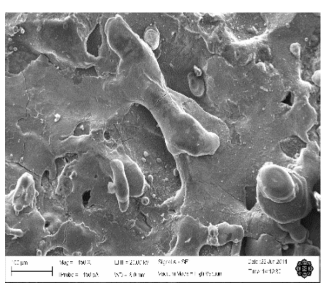

Sl N. 10

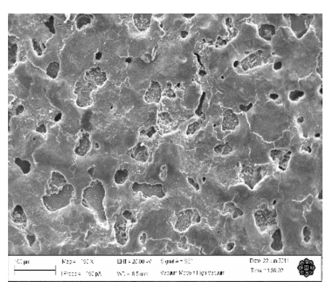

Sl N. 11

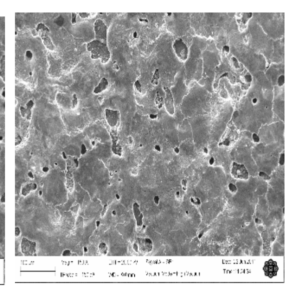

Sl N. 12

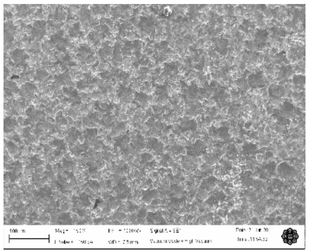

Sl N. 13

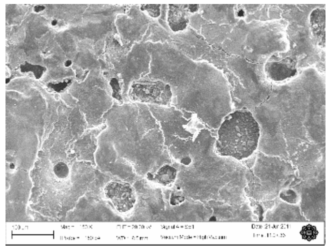

Sl N. 14

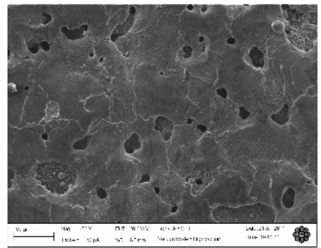

Sl N. 15

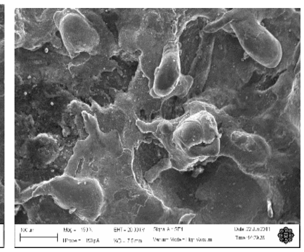

Sl N. 16

(a) Ti-15V-3Al-3Cr-3Sn

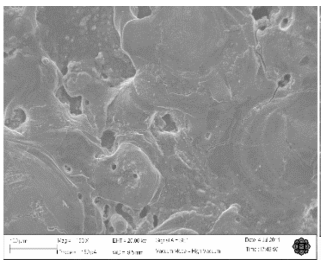

Sl N. 17

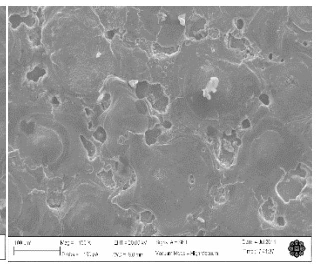

Sl N. 18

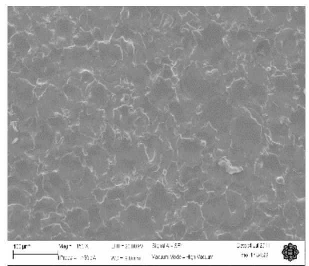

Sl N. 19

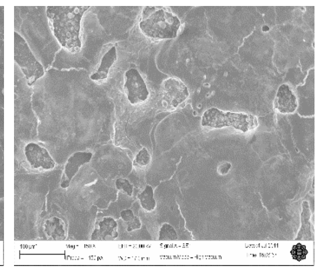

Sl N. 20

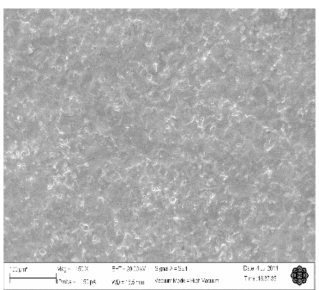

Sl N. 21

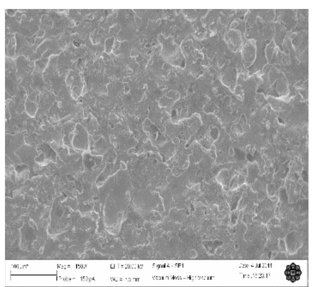

Sl N. 22

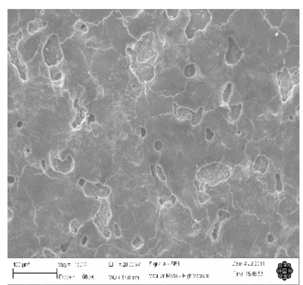

Sl N. 23

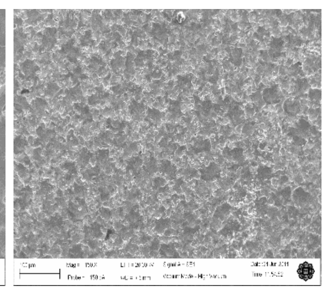

Sl N. 24

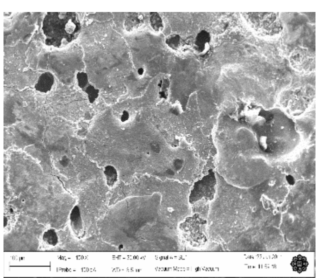

Sl N. 25

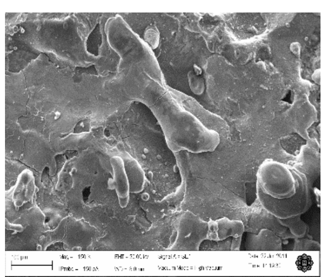

Sl N. 26

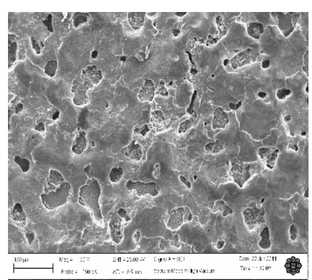

Sl N. 27

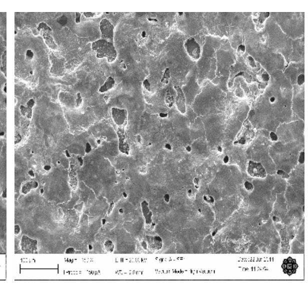

Sl N. 28

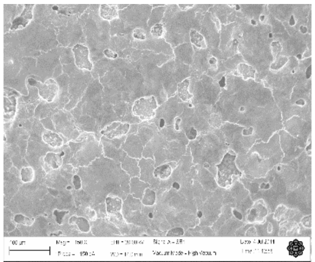

SI N. 29

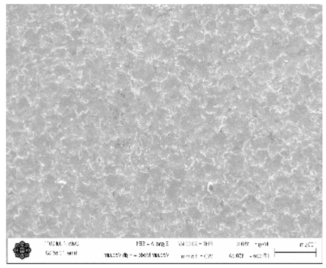

SI N. 30

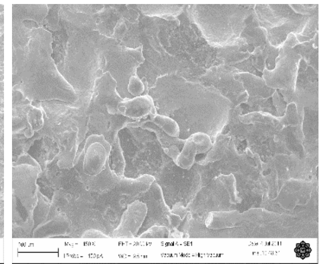

SI N. 31

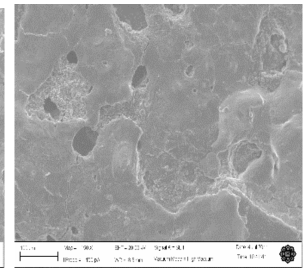

SI N. 32

(b) Ti-6Al-4V

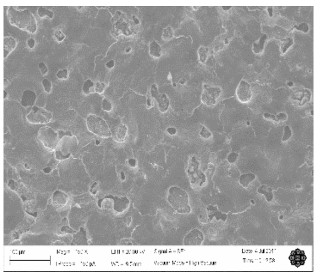

SI N. 33

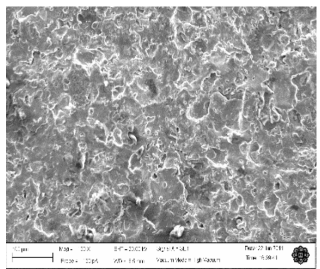

SI N. 34

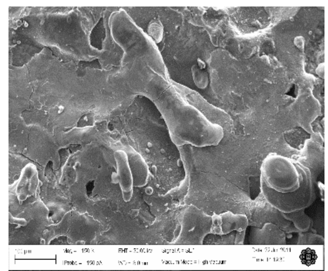

SI N. 35

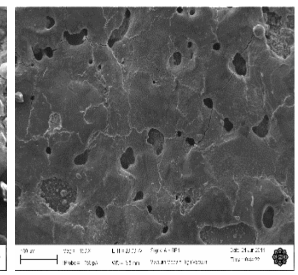

SI N. 36

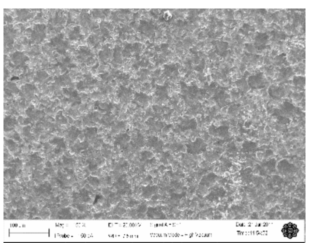

SI N. 37

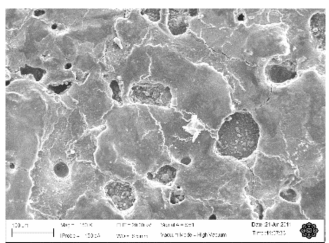

SI N. 38

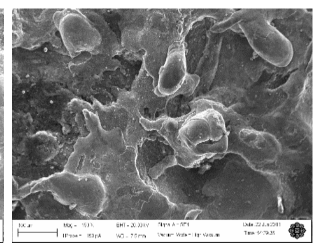

SI N. 39

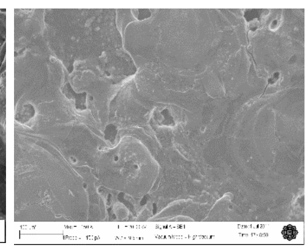

SI N. 40

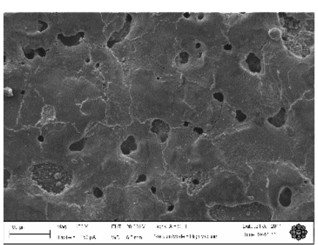

SI N. 41

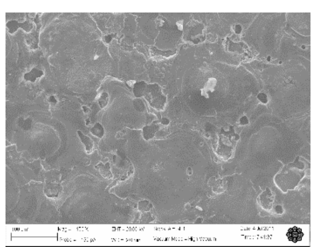

SI N. 42

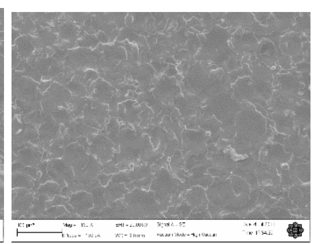

SI N. 43

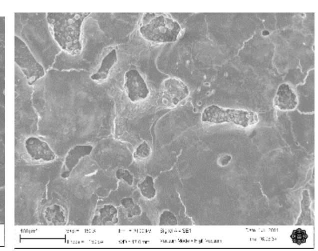

SI N. 44

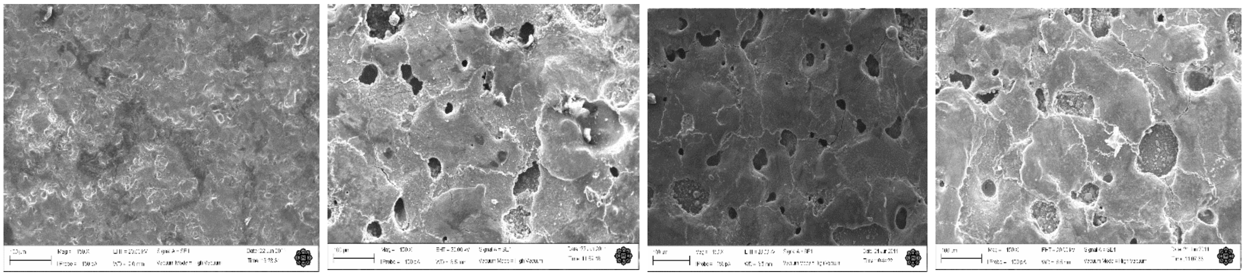

Sl N. 45 Sl N. 46 Sl N. 47 Sl N. 48

(c) Ti-5Al-2.5Sn

Figure 3.2: SEM images of surface roughness of 150x magnification with permission [39-48]

Both positive and negative polarity on different peak currents and pulse on time of three electrodes (Cu, CuW, Gr) provide several values of SR of Titanium alloy materials (Ti-5Al-2.5Sn, Ti-6Al-4V, and Ti-15V-3Al-3Cr-3Sn). We have used 70x3 sets of images with three different magnification ranges (100x, 150x, 500x). Table 3.1 shows the machining parameters applied to generate all the raw images.

Table 3.1: Data parameter details with their corresponding surface roughness values

Input					Output
Serial No.	**Electrical Discharge**	**Electric Polarity**	**Electrode/ Cutting Tool**	**Machined Material**	**Surface Roughness value**
1	2x95	Positive	Cu	Ti-6Al-4V	1.1426
2	2x95	Positive			1.1426
3	15x180	Positive			2.7428
4	15x180	Positive			2.7428
5	29x320	Positive			4.6424
6	29x320	Positive			4.6424
7	2x95	Negative			1.0248
8	15x180	Negative			4.8958
9	29x320	Negative			6.2772
10	2x95	Positive	CuW		0.0958
11	15x180	Positive			3.4286
12	29x320	Positive			5.3345
13	2x95	Negative			1.0633
14	15x180	Negative			4.5272
15	29x320	Negative			6.8408
16	2x95	positive	Gr		1.2946
17	15x180	positive			4.5176
18	29x320	positive			6.4377
19	2x95	Negative			3.1762
20	2x95	Negative			3.1762

21	2x95	Positive	Cu	Ti-5AI-2.5Sn	0.9862
22	2x95	Positive			2.7543
23	15x180	Positive			5.2134
24	15x180	Positive			1.0593
25	29x320	Positive			4.728
26	29x320	Positive			6.7334
27	2x95	Negative			0.8315
28	15x180	Negative			3.0652
29	29x320	Negative			6.3067
30	2x95	Positive	CuW		1.069
31	15x180	Positive			4.3732
32	29x320	Positive			4.728
33	2x95	Negative			6.7334
34	15x180	Negative			0.8315
35	29x320	Negative			3.0652
36	2x95	positive	Gr		6.3067
37	15x180	positive			1.2745
38	29x320	positive			2.7233
39	2x95	Negative			6.5832
40	2x95	Negative			3.4354
41	2x95	Positive	Cu	Ti-15V-3Al-3Cr-3Sn	3.006
42	2x95	Positive			10.0762
43	15x180	Positive			16.9217
44	15x180	Positive			1.5411
45	29x320	Positive			4.7107
46	29x320	Positive			6.8276
47	2x95	Negative			1.0458
48	15x180	Negative			4.8196
49	29x320	Negative			7.0775
50	2x95	Positive	CuW		1.0458
51	15x180	Positive			4.847
52	29x320	Positive			5.2655
53	2x95	Negative			1.1985
54	15x180	Negative			4.7185
55	29x320	Negative			6.6521
56	2x95	positive	Gr		0.853
57	15x180	positive			3.434
58	29x320	positive			4.7288
59	2x95	Negative			1.0488
60	15x180	Negative			0.853

3.4 DATA PREPROCESSING

Image preprocessing is an important step that involves a set of strategies to prepare digital images to be examined or undergo some other calculations. This is to filter out any unnecessary data that must be provided so that the model results in maximum accuracy. In this case, the most important steps can be described as image cropping, data augmentation, storing enhanced images, and splitting a dataset into smaller groups. Augmentation is the methodology in image processing that introduces variations of the image using transformations (such as scaling, zooming, rotating, adjusting brightness or contrast, etc.). The method typically multiplies the dataset by copying image data, producing modified copies. We have augmented the original images separately at three magnifications. We have 3709 augmented images. The values in the filenames were extracted systematically, in the case of surface roughness. Stratified random sampling was used to break each of the datasets into training, validation, and testing. These steps of preprocessing are sequentially described in Figure 3.3.

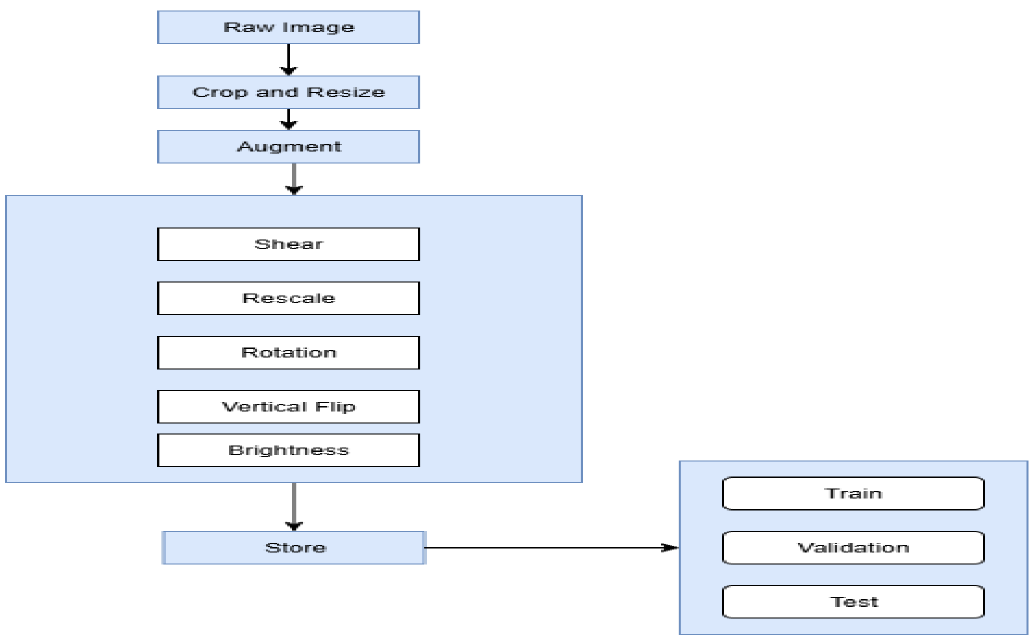

Figure 3.3: Image preprocessing steps

3.5 AI MODEL DEVELOPMENT TO PREDICT SR

We want to predict the surface roughness value for any machined image. For now, we have only machined SEM images with their roughness values as a dataset. For this study, we have used 100x, 150x, and 500x magnifications. The implemented models on these three magnifications are**:**

A. CNN-based Deep Learning models for regression, where we have implemented **–**

   1. Simple Custom CNN Model

2. Resnet50 Model
3. Visual Geometry Group Of The University Of Oxford Model 16 (VGG16)

B. Moderated methods with -

1. Support Vector Regression
2. Random Forest Regression and
3. Linear regression.

We have used three different magnification datasets- 150x, 100x, and 500x for each of the models separately. We will use these magnifications for each model and will compare the models.

3.5.1 CNN-Based Deep Learning Models For Regression

The processing of SEM images is performed by loading a folder with images into the program and preprocessing it with a suitable conversion (1. /255) and normalization. The code first obtains the labels of the TIFF image filenames that contain the information about the surface roughness and constructs a Data Frame. The get roughness as given in the file name method divides all the file names on underscores and converts the second expression to a floating-point number (roughness value). It also caters to errors by giving a none. It shifts .tiff files in the directory, runs the function of extracting the roughness value, and ties valid dataset names with the corresponding roughness value. A pandas DataFrame is made of column names, filename, and roughness, which throws an error when invalid data does not exist. This is the data preparation before model training.

(1) Simple Custom CNN Model Architecture

The custom CNN was created in TensorFlow and the Keras API to operate on the grayscale images. The architecture consists of:

- Convolutional Layers: The convolutional layers perform the first valuable step of feature extraction by applying filters (kernels) to the input images. The succeeding layers comprise filters that enable the model to identify various surface textures. Convolutions are followed by max-pooling layers whose goal is to minimize the dimensions of the feature map, preserving the most crucial information to enhance the computational effectiveness. With the number of filters (density filters) at the respective layers being 32, 64, 128, and 256; a 2x2 dimensionality reducing max-pooling; a kernel size of 3x3 and ReLU activation: This comprises four layers.

- Fully Connected Layers: Out of the feature extraction process, the feature maps are then connected to the flattened layer. The flatten layer accepts the multi-dimensional data (provided by the convolution and pooling layers) and transforms it into a one-dimensional vector. Dropout layers are applied in different layers of the network to avoid overfitting. In this model, there will be the Flatten layer, dense layer (ReLU activation), dropout layer to prevent overfitting, and dense layer (no activation) to regress.

Compilation: Mean Squared Error (MSE) loss, Adam optimizer, and Mean Absolute Error (MAE) are other quantities to compile the model.

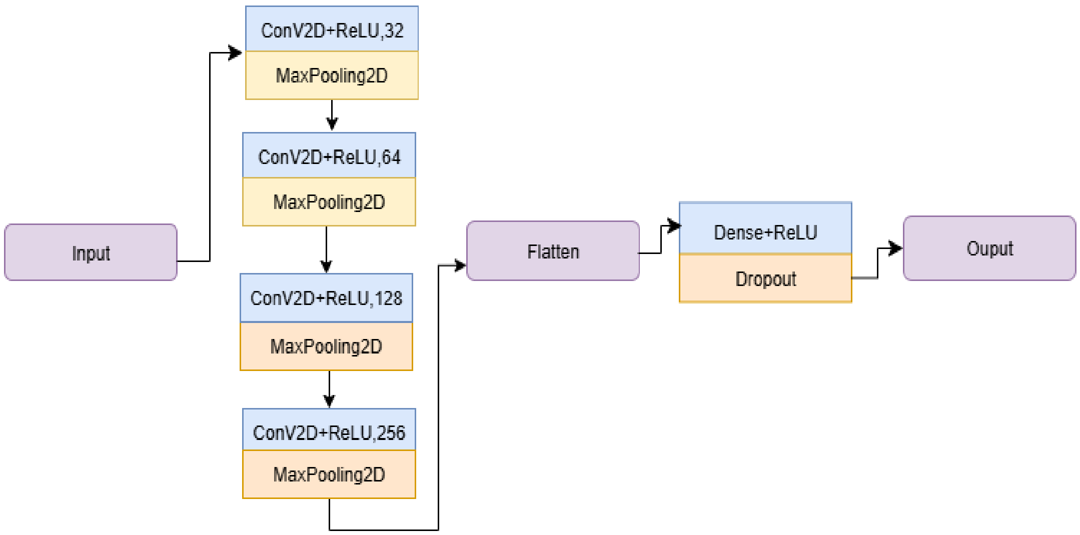

Figure 3.4: CNN Model Architecture

(2) Resnet50 Model Architecture

Microsoft Research proposed ResNet-50, a convolutional neural network with 50 layers in 2015, to solve vanishing gradient problems of deep networks. It employs residual connection, and this enables the network to approximate residual functions, making it easy and efficient to train deep networks. It was the pretrained ResNet50 model that was initially trained on ImageNet, adapted to regression. Such a model was adjusted by:

- Instead of the top layer of the classification, a global average-pooling layer is used, and then a dense layer containing 256 units (ReLU activation), a 50 percent dropout layer, and a single-unit dense layer (regression) is added.
- First, freezing the convolutional base and fine-tuning some layers (e.g., the last residual block) to adapt to SEM images.
- The compilation was done using MSE loss and Adam optimizer (fine-tuning of initial learning rates).

It was necessary to preprocess the input images to 224x224x3 (RGB) to fit the requirements of ResNet50.

(3) VGG16 Model Architecture

VGG-16 is a simple CNN designed in 2014 by the Visual Geometry Group at Oxford and identified as 16 layers of a convolutional neural network with stacked 3x3 convolutional filters and a uniform architecture. Its simple architecture qualifies it as an efficient feature extraction form, registering about 71% top-1 accuracy on ImageNet.

Being computationally expensive and slow to train, VGG-16 has about 138 million parameters. It is still recent and popular to use in transfer learning and applications such as style transfer, yet its size is quite large, making it not suitable for use in resource-limited applications. The pretrained model VGG16 that was trained on ImageNet was adjusted as well:

- The final classification layer was removed and a flatten layer added with a dense layer of 256 (ReLU activation) units, dense dropout layer of 50 percent, and the final dense layer of one unit.
- The convolutional base was first frozen, and fine-tuning was applied on the final several convolutional layers, in order to capture SEM image characteristics.

Loss of MSE and the Adam optimizer were used to produce the model. Original images were reshaped and preliminarily processed, thus meeting the input demands of VGG16 (of dimension 224 x 224 x 3).

3.6 MODERATED METHODS WITH SUPPORT VECTOR REGRESSION, RANDOM FOREST, AND LINEAR REGRESSION

3.6.1 Image Preprocessing and Traditional Feature Extraction

The required libraries (CV2, Pandas,numpy, scikit-image, os, etc.) are imported, and the images are loaded in grayscale mode using the OpenCV library to decrease the degree of complexity of the computation. To extract features of the surfaces, a function is created. The Otsu adaptive thresholding method converts the images into a binary format. On studying the different techniques, some features were chosen that best suited the images on the surface. The features that were extracted from grayscale copies of the SEM images are:

Features	Description
Max_pore_area	Largest detected pore area in binary image
Pore count	Number of pores detected
Edge Density	Number of edge pixels per mm^2 using Canny edge detection
Mean intensity	Average grayscale intensity of the image
Standard Deviation Intensity	Standard deviation of grayscale intensity
Intensity Range	Difference between max and min intensity
Average Eccentricity	Average shape eccentricity of all detected pores

All features were stored in a structured DataFrame and saved as an Excel file. Then the dataset with actual roughness values was split into training and testing.

3.6.2 Model Development

Three regression models were selected and implemented using scikit-learn:

(I) Support Vector Regression: A versatile model, SVR, by application in SVR () with a default RBF kernel, can recognize non-linear patterns by transforming the problem into a high feature space. In case of image regression, it needs prior feature extraction, which means it is best to be utilized on small to moderate-sized tasks that are of medium complexity.

(II) Random Forest Regression: Random Forest Regression (n_estimators=100, random_state=42) is an ensemble of 100 decision-tree-based models that are used to learn the non-linear relationship and feature interaction. In regard to image regression, it requires pre-extracted features, provides resistance to overfitting, and competent performance on moderately complicated tasks. It is less flexible than end-to-end deep learning models by virtue of the fact that it relies on feature extraction. Although this is more effective than Linear Regression on non-linear patterns, it is still not sufficiently effective in complex regression tasks on images without powerful feature preparation.

(III) Linear Regression: In Linear Regression, used in scikit-learn under the name LinearRegression(), the model suggests a linear correspondence among features and the target and forms a hyperplane to minimize mean squared error. To apply image regression, features must have been previously extracted from an image (e.g., HOG, CNN-based), and thus, image regression cannot operate on raw images; hence, it is a fast, simple baseline for simple patterns. It fails to perform well at non-linear image data, where it must be carefully engineered to meet its linear assumption. It performs worse on tasks like depth estimation or pose regression, where non-linear models are expected, but it is computationally cheap.

3.6.3 Model Training And Evaluation

Each model is trained on the training dataset using the fit method, optimizing model parameters to minimize prediction error. Performance is assessed using a suite of metrics. Metrics are computed for both training and testing sets to evaluate model fit and generalization performance.

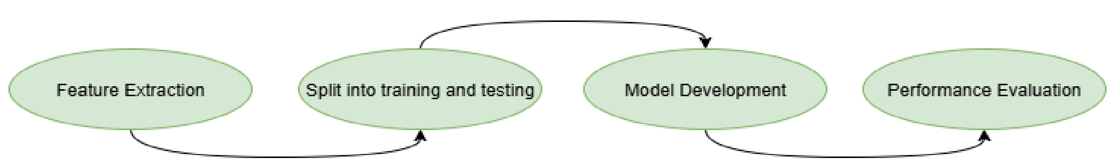

Figure 3.5: Moderated method workflow

3.7 PERFORMANCE EVALUATION

Model performance was evaluated using regression metrics:

i) MSE (Mean Squared Error): MSE is used to measure the average of the squared differences between predicted and actual values. It is used to assess how well the predicted model works. The formula to calculate MAE for a dataset with "n" data points is:

$$MSE = \frac{1}{n}\sum_{i=1}^{n}(xi - yi)2 \qquad (3.1)$$

where:

- xi represents the actual or observed value for the i-th data point.
- yi represents the predicted value for the i-th data point.

ii) MAE (Mean Absolute Error): MAE is calculated as the average of absolute differences between predicted and actual values. The formula to calculate MAE for a dataset with "n" data points is:

$$\text{MAE} = \frac{1}{n}\sum_{i=1}^{n}(xi - yi) \qquad (3.2)$$

where:

- xi represents the actual or observed values for the i-th data point.
- yi represents the predicted value for the i-th data point.

iii) RMSE (Root Mean Squared Error): It is the square of MSE.The formula for RMSE for a dataset with 'n' data points is as follows:

$$\text{RMSE} = \sqrt{\frac{1}{n}\sum_{i=1}^{n}(xi - yi)2} \qquad (3.3)$$

where:

- RMSE is the Root Mean Squared Error.
- xi represents the actual or observed value for the i-th data point.
- yi represents the predicted value for the i-th data point.

iv) R^2 (R-squared): It is also called the coefficient of determination. It indicates the proportion of the variance in the dependent variable that is predictable from the independent variables. It's a measure of model fit. The formula to calculate the R-squared score is as follows:

$$R^2 = 1 - SSR/SST \qquad (3.4)$$

where:

- R^2 is the R-squared.
- SSR represents the sum of squared residuals between the predicted values and actual values.
- SST represents the total sum of squares, which measures the total variance in the dependent variable.

3.8 IMAGE PROCESSING TOOLS

This study suggests the application of a diverse set of open-source and freeware tools that are broadly accepted in research and development in implementing the suggested system. A summary of some of the tools deployed is given below:

• Python: Python is a high-level programming language with support for object-oriented programming, but it is best suited to modular and scalable programs.

• Pandas: A Python library that can offer a strong data structure to manipulate and analyze relational or labeled data effectively.

• NumPy: It is one of the basic Python libraries that provides array support and provides support for mathematical operations such as random number generation, operations in linear algebra, and the Fourier transform.

• Matplotlib: It is a Python program that is a visualization library mainly utilized to create fixed, dynamic, and interactive pictures of data that are beneficial in the analysis and presentation of the data.

• OpenCV: An open-source, comprehensive library for conducting computer vision, machine learning, and image processing, which allows a person to perform sophisticated tasks on images and videos.

• TensorFlow: A machine learning framework that offers a flexible model and is open-source for constructing and training a deep learning architecture.

• Keras: a convenient high-level API on top of TensorFlow with simple development, focusing on ease of use and experimentation.

• Google Colab: It is a Jupyter notebook that does not need any setup to utilize, and offers an opportunity to access computing resources, such as GPUs, at no cost.

All these create a strong basis of the system that facilitates effective development, processing, and analysis in the case of this research.

3.9 SUMMARY

Here we have talked about the methodology of the surface roughness measured by Convolutional Neural Network regression and the moderate method with classic feature extraction in SEM images. It involves creating a CNN, having convolutional, maxpooling, and fully connected layers, and training it on the entire dataset. Resnet50 and VGG16 pretrained models are also used to be analyzed. Our approach is generalizable and can be applied to many tasks in image classification, increasing the accuracy and performance of automated systems based on images. The moderate method we have applied is using a variety of models- Linear regression, random forest regression, and SVR.

CHAPTER 4

RESULTS AND DISCUSSION

4.1 INTRODUCTION

In this chapter, we will present the study's results and discuss how the study's aim predicted the surface roughness of titanium alloys from SEM images. We have given the result of the AI models to predict SR for the magnification 150x in section 4.2. Then, in section 4.3, we have provided the result for magnification 100x. Then we have provided the results for magnification 500x in section 4.4. We have shown testing results for unknown images in section 4.5, and at the end of this chapter, we have discussed the comparison of the dataset models.

4.2 AI MODELS TO PREDICT SR FOR 150x MAGNIFICATION DATASET

Result analysis refers to the act of analyzing the performance and results of a system or a process by using data. With the help of the study, we can predict the roughness of the machined surface of the titanium alloys using SEM photos. Each of the three Convolutional Neural Network models, custom CNN, ResNet50, VGG16, and moderate methods with SVR, RF, and LR, was used to evaluate and compare their performance on three datasets. In all the models, there are 1400 images in the dataset of 150x magnification (1011 images are trained, 179 images are validation, and 210 images are testing).

4.2.1 CNN-Based Deep Learning Models For Regression for 150x Magnification Images

Images of magnification 150x have been used to train three kinds of CNN-based Deep Learning models trained to perform Regression. Image filenames were used to extract the value of surface roughness, and this value was saved to a DataFrame. The feature extraction and model training were performed after the normalization of the SEM images.

1. Simple Custom CNN Model

Training Result

The training output is the extent to which the model has been trained to produce accurate predictions in the training data. The custom CNN was trained on 100 epochs with the training and validation loss plots. The model has reached 66 epochs due to the early stopping because the validation score has not improved over 0.04683. The final training loss was 0.0482, and the final training MAE was 0.1604; the corresponding validation loss was 0.0486, and the validation MAE was 0.1618.

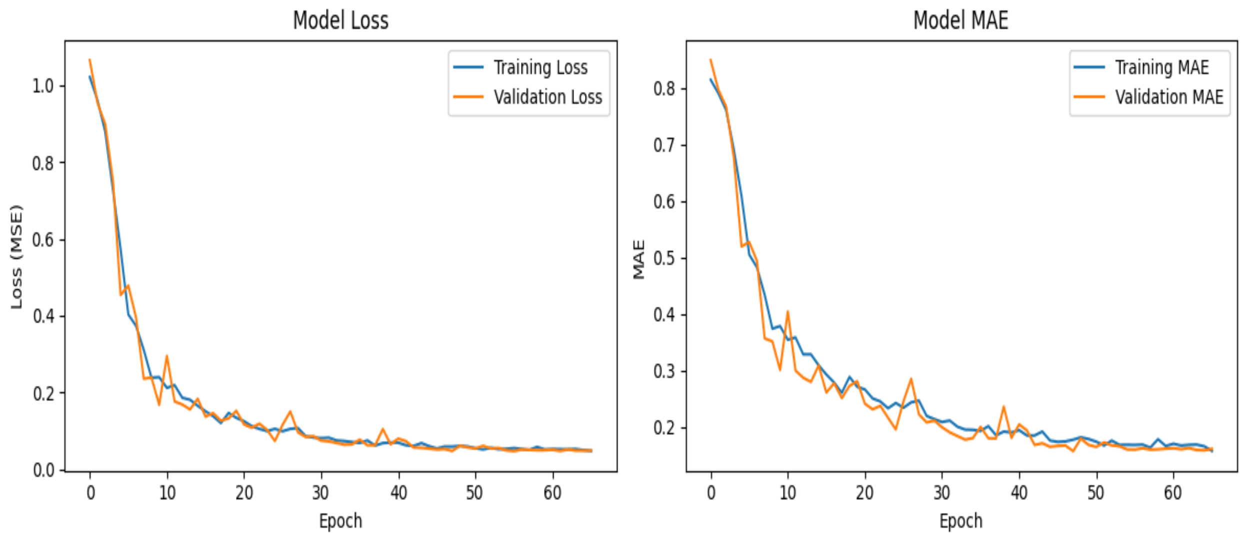

Figure 4.1: Training vs validation graph of a simple custom CNN of 150x

The training loss will give an idea of how close we have become to the data in our training data set, and the validation loss will tell us how accurately our model can be used with data not included within the training set. Both measures are important in the performance of a machine-learning model and averting overfitting. Validation loss and training loss are well related in this graph; as a consequence, overfitting is not a big issue.

Testing Result.

After training the model on the training set and the subsequent optimization of the loss function, the model is tested on the test set to check its performance on a total of 210 images. The actual output is normally presented in the form of a variety of evaluation indicators, e.g., MSE, RMSE, MAE, and R^2, which are the indicators applied to compare the results of various models or to show how a model fares on a defined task.

MSE: 0.1684

RMSE: 0.4103

MAE: 0.2763

R^2: 0.9498

The custom CNN showed an MSE of 0.1684, RMSE of 0.4103 µm, MAE of 0.2763 µm, and R^2 = 0.9498 on the test set. These statistics suggest that the model explains 94.98 percent of the variance in the roughness of surfaces, and its predictive error is, on average, 0.2763 µm.

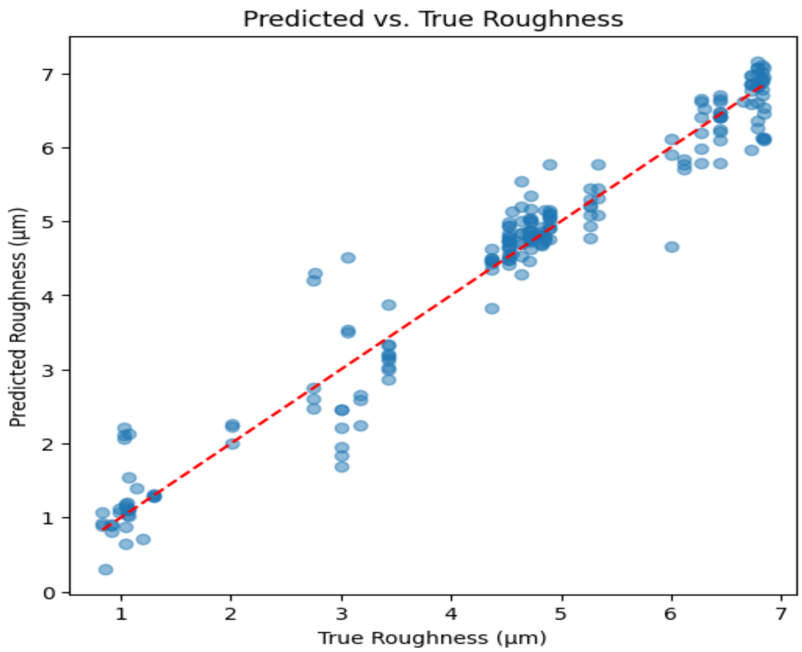

Figure 4.2: Actual vs predicted result of a simple CNN of 150x

The regression plot of the predicted and the actual roughness values indicates a strong linear relationship, with most of the predictions approximately along the dissection line, as well as the existence of minor outliers to indicate difficulty in predicting high and low roughness values.

2. ResNet50 Model

Training Result

The ResNet50 model with pretrained ImageNet weights was trained during 100 epochs, reaching the final loss values of 0.5080 and validation MAE of 0.5400. As displayed in the training log, there is a gradual development, with the validation loss reading 0.5104 at epoch 97, recording a decrease of 0.5080 at epoch 100, which means slow but stable adaptation to a SEM image domain.

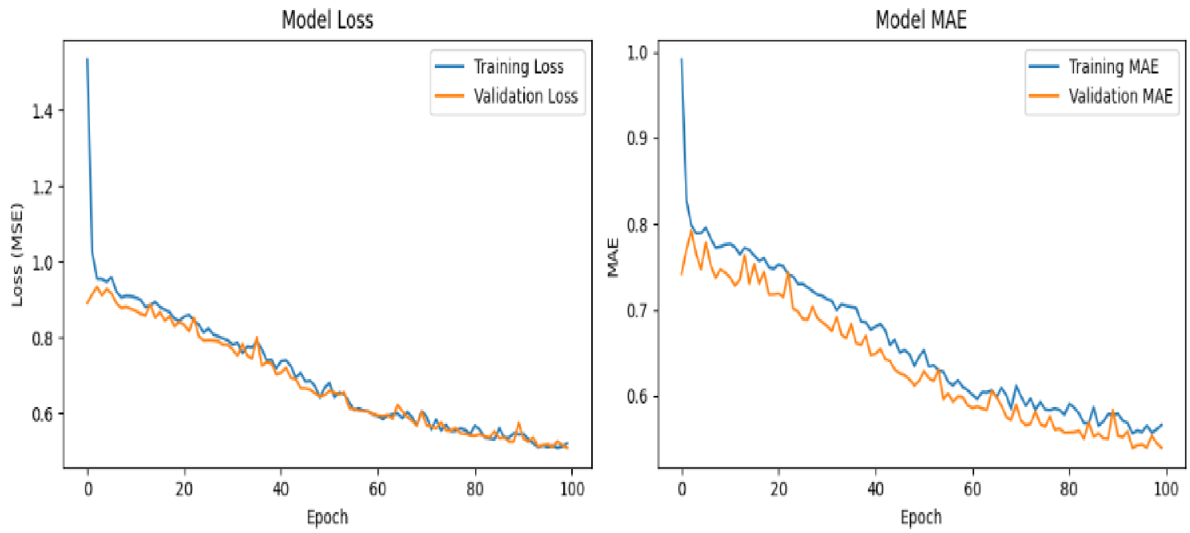

Figure 4.3: Training vs validation graphs of Resnet50 of 150x

The graphs of the MAEs show a slow decline, but the relatively large validation MAE hints that ResNet50 has not been helpful in grasping the more subtle texture details of 150x SEM images fully.

Testing Result

The results of performance metrics are-

MSE: 1.8649
RMSE: 1.3656
MAE: 1.0346
R^2: 0.4698

ResNet50 produced an MSE of 1.8649, RMSE of 1.3656 µm, MAE of 1.0346 µm, and R^2 of 0.4698 on the test set. These findings reveal that the model contributes to explaining the variance in the values of roughness of only 46.982, with a high average error.

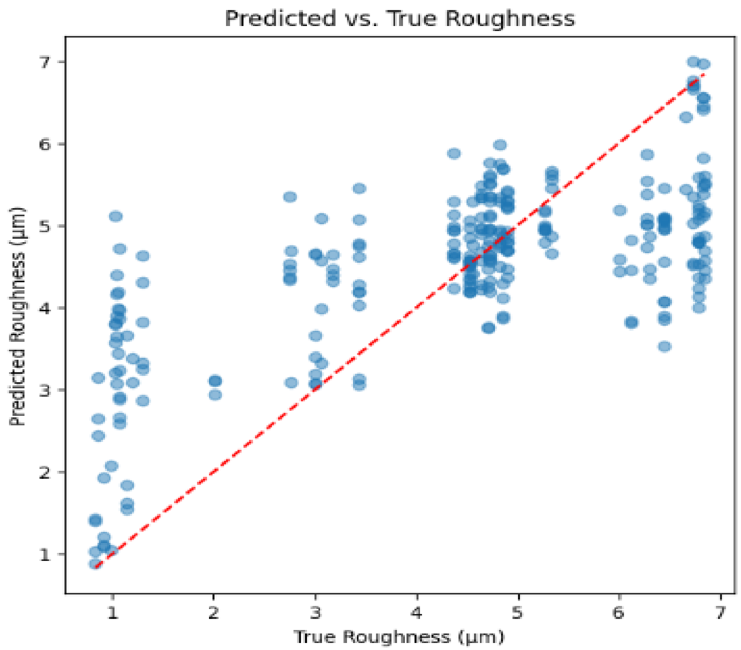

Figure 4.4**:** Actual vs predicted graph of Resnet50 of 150x

The scatter plot is likely to be highly scattered, indicating the poor predictive accuracy and the difficulty the model would have in terms of generalizing to the test data, as the Resnet50 model is trained on RGB images, but we are using grayscale images in this model.

3. VGG16 Model

Training Result

VGG16, which was trained on ImageNet, had an outstanding training speed, and training and validation loss curves closed quickly, at 20-30 epochs. Training and validation loss were very similar, with minimal overfitting, but displayed great generalization.

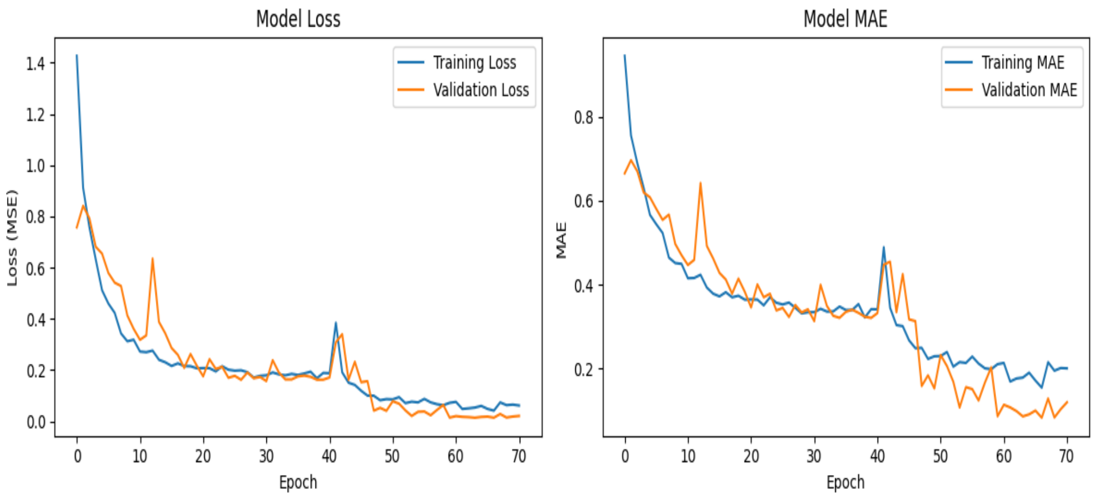

Figure 4.5**:** Training vs validation plots of VGG16 of 150x

The MAE curves indicate that the performance rapidly decreases, followed by stable optimization, which indicates an effective learning of the features of the surface roughness by VGG16. The combination of pre-trained weights and fine-tuning of the last convolutional layers allowed quick adaptation to 150x SEM images.

Testing Result

VGG16 was the most successful due to an MSE of 0.0509, RMSE of 0.2257 m, MAE of 0.1660 m, and R^2 of 0.9855 on the test set. These outcomes show that VGG16 covers 98.55 per cent of the variance in values of roughness with a small mean error of 0.1660 micrometers.

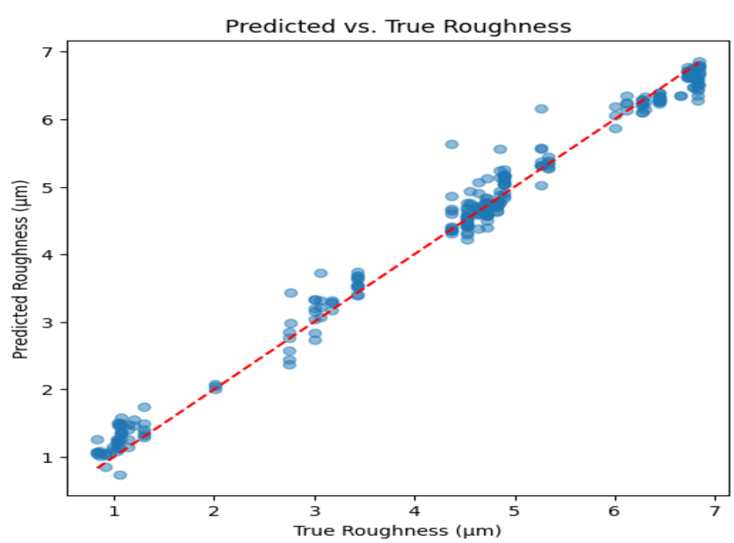

Figure 4.6: Actual vs Predicted result of VGG16 of 150x

The scatter plot indicates a close distribution of predictions around the line of equality, which once again proves the high level of accuracy and consistency of VGG16 with 150x magnification SEM images.

4.2.2 Moderated Methods using 150x Magnification Images

Images of SEM were transformed into grayscale form and binarized. Based on them, such surface features as the maximum pore area, the number of pores, the density of edges, and intensity-related features were extracted.

1. Support Vector Regression Model

To predict the roughness of a surface, the Support Vector Regression model was trained on the extracted features of SEM images at 150x magnification. The model managed to reach-

Training - MAE: 0.81, MSE: 1.35, RMSE: 1.16, R^2: 0.68

Testing - MAE: 1.02, MSE: 1.86, RMSE: 1.36, R^2: 0.58

Cross-Val R^2: 0.56

The traditional way of extracting equivalent features was to transform an SVR model into a nonlinear relation using a radial basis function kernel. It possessed a training R^2 of 0.68, a test R^2 of 0.58, and a cross-validation R^2 of 0.56, indicating a moderate and repeatable performance.

2. Random Forest Regression Model

Random Forest Regression model was applied to the extracted surface features based on 150x magnification SEM images

Band: MAE: 0.26, MSE: 0.17, RMSE: 0.41, R^2: 0.97

Testing - MAE: 0.70, MSE: 1.07, RMSE: 1.04, R: 0.76

Cross-Val R^2: 0.74

The features that were conventionally extracted and achieved high levels of interaction through the usage of the Random Forest were the pore count and the measures of intensity. It also possessed a great training R^2 of 0.95, test R^2, and cross-validation R^2 of 0.76 and 0.74, respectively, with desirable generalization.

3. Linear Regression Model

A Linear Regression model was developed with the results of feature extraction on SEM images at a magnification of 150x, which was used to forecast surface roughness. The training of the model and its testing were done by training, testing, and cross-validation to test its predictive values.

Training - MAE: 1.40, MSE: 2.81, RMSE: 1.68, R^2: 0.33

Testing - MAE: 1.42, MSE: 2.82, RMSE: 1.68, R^2: 0.37

R^2 Cross-Val: 0.31

Linear Regression has been a benchmark model, which, in terms of the traditionally identified features (porosity and edge density), dealt with a linear dependent relationship with Actual Roughness. With low R^2 values of 0.33 and 0.37 during the training and testing, it might not fit well the trend of SEM images data that is inherently complicated and nonlinear.

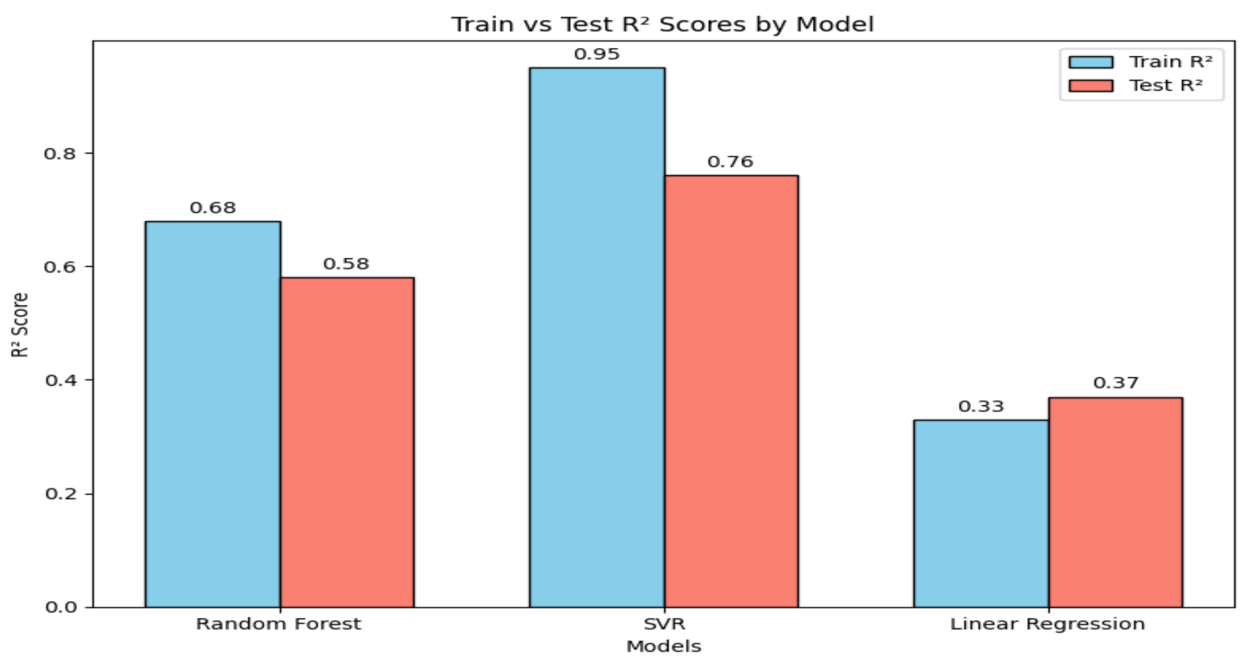

Figure 4.7 : Train vs test R^2 for three models of 150x magnification

4.3 AI MODELS TO PREDICT SR FOR 100x MAGNIFICATION DATASET

The dataset of 100x magnification, comprising 1200 images, is split into training (867 images), validation (153 images), and testing (180 images), and is applied as input to all AI models.

4.3.1 CNN-Based Deep Learning Models for Regression for 100x Magnification Images

Images of magnification 100x have been used to train three kinds of CNN-based Deep Learning models trained to perform Regression. Image filenames were used to extract the value of surface roughness, and this value was saved to a DataFrame. The feature extraction and model training were performed after the normalization of the SEM images.

1. Simple Custom CNN Model

Training Result

Training result is the measure of how successfully the model has captured the training data to make accurate predictions. A custom CNN was trained in 100 epochs, and training and validation loss curves were observed. Training loss was minimized to 0.0724 and MAE 0.2103, and the validation loss was 0.0483 and val_MAE 0.1677. The training and validation loss are closely related. Thus, the overfitting issue is not significant.

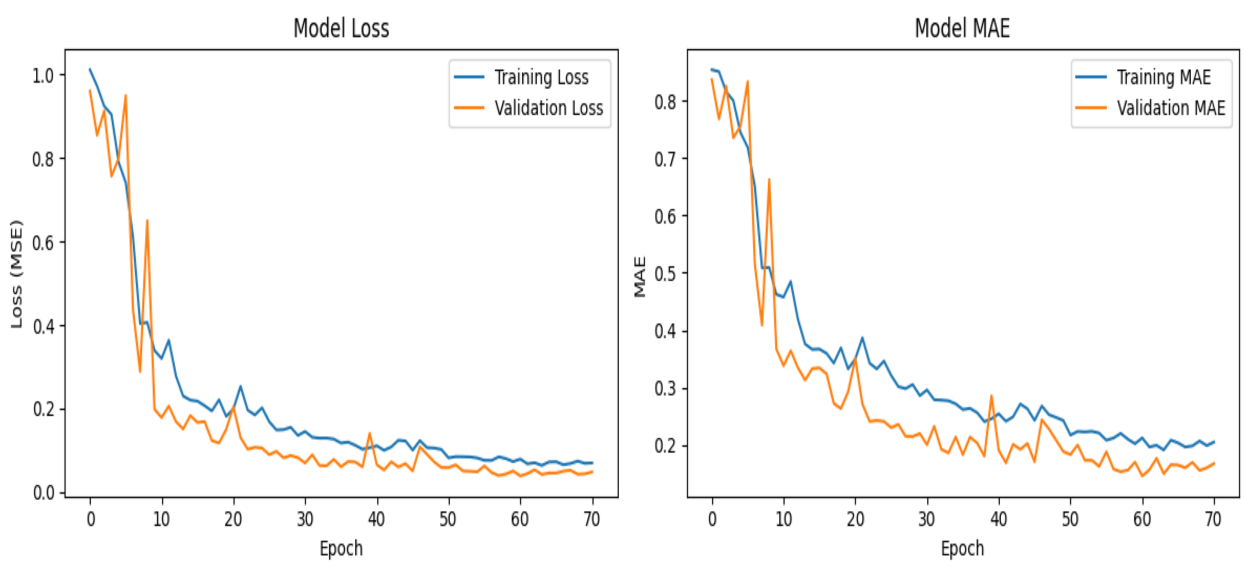

Figure 4.8: Training vs validation plots of a simple CNN of 100x

Testing Result

After training the model on the training set, and keeping it tuned to minimize loss, it is assessed on the test set to gauge its accuracy in ranking the test set of a total of 180 images, which are unseen by the model. It is common to report the result of the test with a set of evaluation metrics, e.g., MSE, RMSE, MAE, and R^2. These are used to compare the behavior of different models or to assess the behavior of a model on a given task.

MSE: 0.1738

RMSE: 0.4169

MAE: 0.2965

R^2: 0.9623

The custom CNN showed an MSE of 0.1738, RMSE of 0.4169 μm, MAE of 0.2965 μm, and R^2 = 0.9623 on the test set. These statistics suggest that the model explains 96.23 percent of the variance in the roughness of surfaces, and its predictive error is, on average, 0.2965 μm.

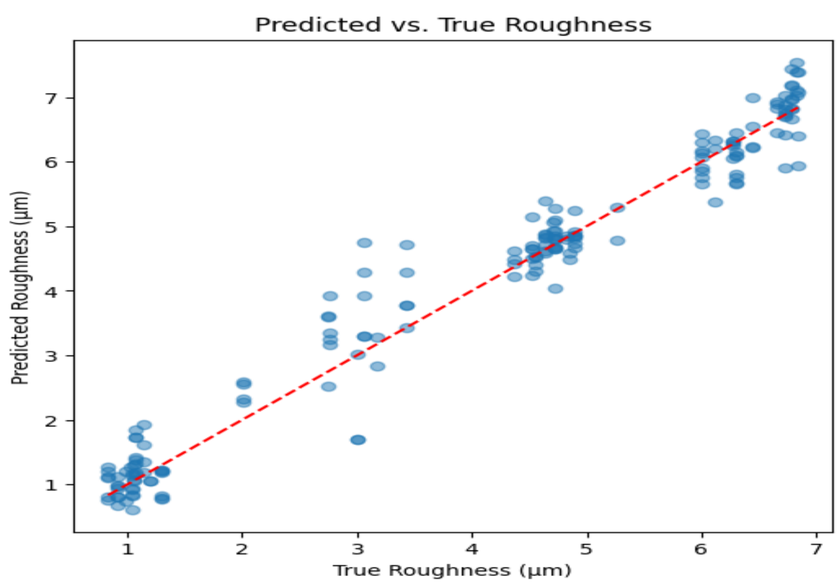

Figure 4.9: Actual vs predicted result of a simple custom CNN of 100x

The regression plot of the predicted and the actual roughness values indicates a strong linear relationship, with most of the predictions approximately along the dissection line, as well as the existence of minor outliers to indicate difficulty in predicting high and low roughness values.

2. ResNet50 Model

Training Result

The ResNet50 model with pertained ImageNet weights was trained during 100 epochs, reaching the final loss values of 0.7172 and a validation loss of 0.5630. The model runs for 100 epochs.

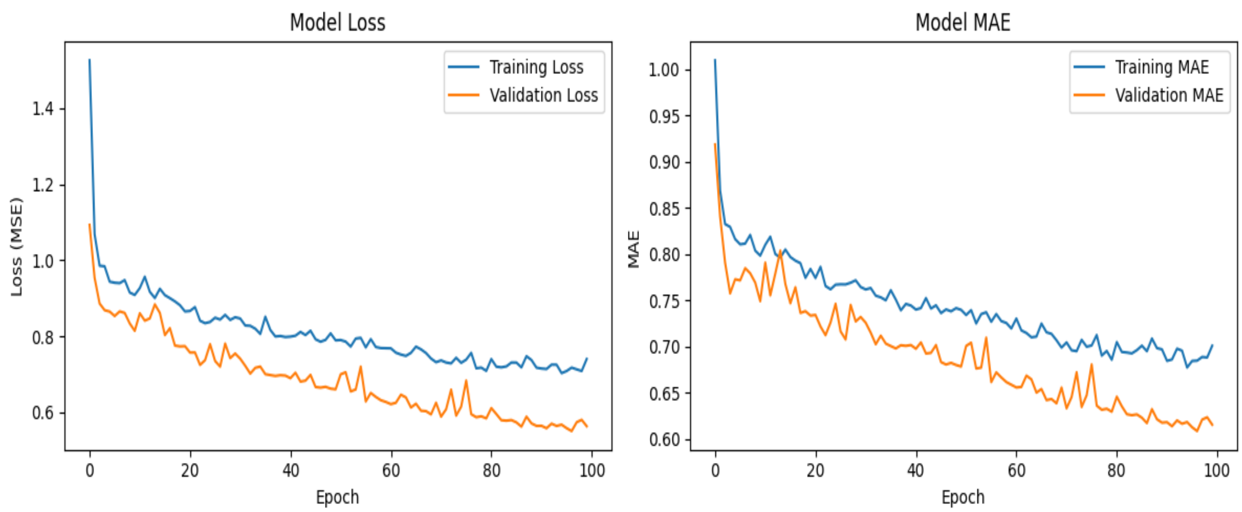

Figure 4.10: Training vs validation of ResNet50 of 100x

From the graphs, we can see that ResNet50 has not been useful in grasping the more subtle texture details of 100x SEM images.

Testing Result

The results of performance metrics are-

MSE: 2.8266
RMSE: 1.6812
MAE: 1.3636
R^2: 0.3504
ResNet50 produced an MSE of 2.8266, RMSE of 1.6812 µm, MAE of 1.3636 µm, and R^2 of 0.3504 on the test set. These findings reveal that the model contributes to explaining the variance in the values of roughness of only 35.04, with an average error that is quite high.

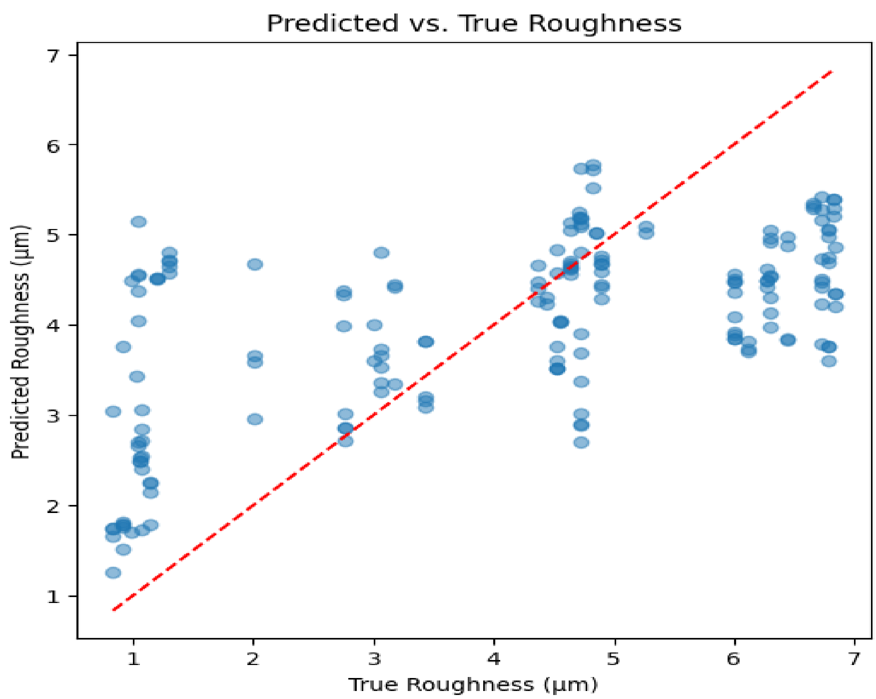

Figure 4.11**:** Actual vs predicted plot of ResNet50 of 100x

The scatter plot is likely to be highly scattered, indicating the poor predictive accuracy and the difficulty the model would have in terms of generalizing to the test data, as the Resnet50 model is trained on RGB images, but we are using grayscale images in this model.

3. VGG16 Model

Training Result

The regression model using the VGG16 architecture recorded a consistent decline in the loss of training and validation as the epoch passed. In the early stages of training, the validation MAE decreased rapidly, going down to 0.33 in the first 25 epochs. The minimum validation loss of 0.0477 and MAE of 0.1727 occurred at epoch 34, which indicates the good capacity of the model to predict the SEM image to surface roughness very accurately. This experiment shows the success of transfer learning on VGG16 applied to Regression in the scope of microstructure image analysis.

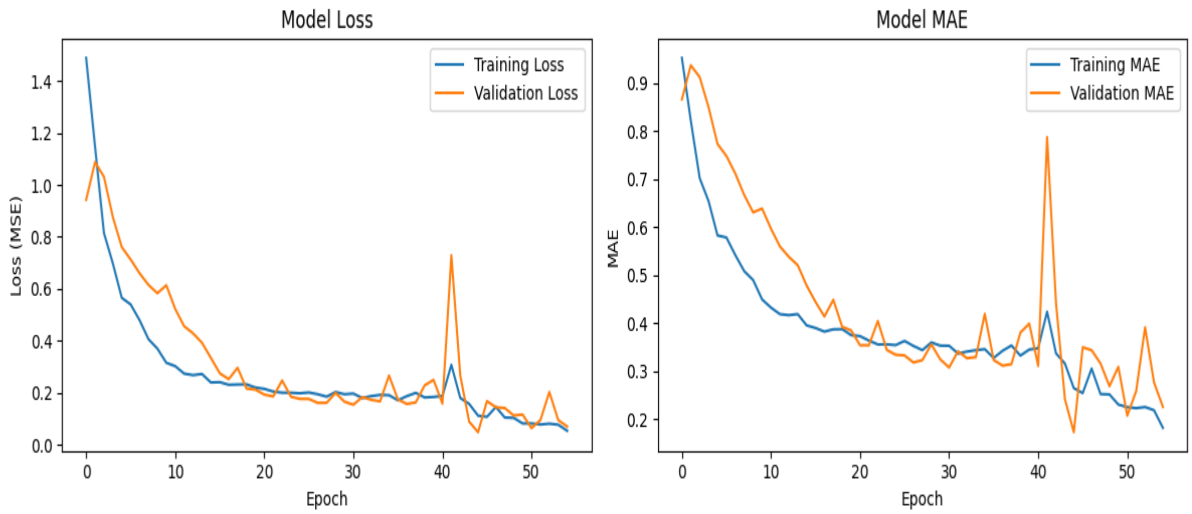

Figure 4.12: Training vs validation plots of VGG16 of 100x

The MAE curves indicate that the performance rapidly decreases, followed by stable optimization, which indicates effective learning of the surface roughness features by VGG16. The combination of pre-trained weights and fine-tuning of the last convolutional layers allowed quick adaptation to 100x SEM images.

Testing Result

VGG16 was successful due to an MSE of 0.1981, RMSE of 0.4451 m, MAE of 0.3520m, and R^2 of 0.9560 on the test set. These outcomes show that VGG16 covers 95.60 percent of the variance in values of roughness with a small mean error of 0.3520 micrometers.

MSE: 0.1981
RMSE: 0.4451
MAE: 0.3520
R^2: 0.9560

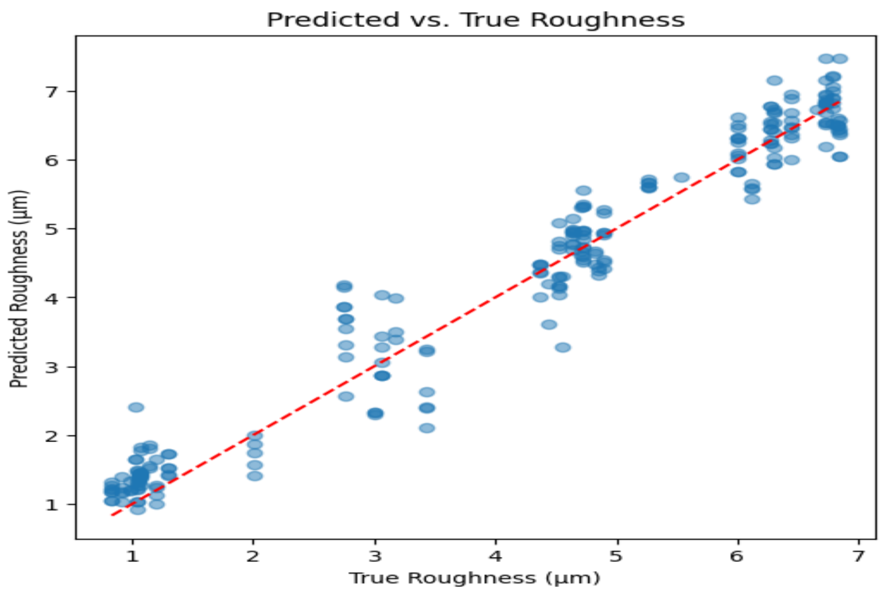

Figure 4.13: Actual vs predicted plot of VGG16 of 100x

The scatter plot indicates a close distribution of predictions around the line of equality, which once again proves the high level of accuracy and consistency of VGG16 with 100x magnification SEM images.

4.3.2 Moderated Methods using 100x Magnification Images

Images of SEM were transformed into grayscale form and binarized. Based on them, such surface features as the maximum pore area, the number of pores, the density of edges, and intensity-related features were extracted.

1. Support Vector Regression Model

To predict the roughness of a surface, the Support Vector Regression model was trained on the extracted features of SEM images at 100x magnification. The model managed to reach-

Training - MAE: 0.75, MSE: 1.14, RMSE: 1.07, R^2: 0.71

Testing - MAE: 0.88, MSE: 1.53, RMSE: 1.24, R^2: 0.60

Cross-Val R^2: 0.63

SVR is performing decently, although it cannot compete with RF based on its training R^2 of 0.71, test R^2 of 0.60, and cross-validation R^2 of 0.63, allegedly due to sensitivity in response to the intricate characteristics or hyper-parameter settings.

2. Random Forest Regression Model

Random Forest Regression model was applied to the extracted surface features based on 100x magnification SEM images.

Training - MAE: 0.26, MSE: 0.17, RMSE: 0.42, R^2: 0.96

Testing- MAE: 0.50, MSE: 0.62, RMSE: 0.79, R^2: 0.84

Cross-Val R^2: 0.77

RF could capture the complicated interactions based on the traditionally retrieved features, such as pore counts and intensities. It can fit well to training and provide powerful generalization with training $R^2 = 0.96$, testing $R^2 = 0.84$, and cross-validation $R^2 = 0.77$.

3. Linear Regression Model

A Linear Regression model was developed with the results of feature extraction on SEM images at a magnification of 100x, which was used to forecast surface roughness. The training of the model and its testing were done by training, testing, and cross-validation to test its predictive values.

Training - MAE: 1.27, MSE: 2.56, RMSE: 1.60, R^2: 0.34

Testing- MAE: 1.21, MSE: 2.56, RMSE: 1.60, R^2: 0.32

Cross-Val R^2 : 0.31

When using LR as a reference, a traditional benchmark produces linear associations using the obtained features. It can hardly select complex patterns due to the low value of R^2 (0.34 training, 0.32 testing).

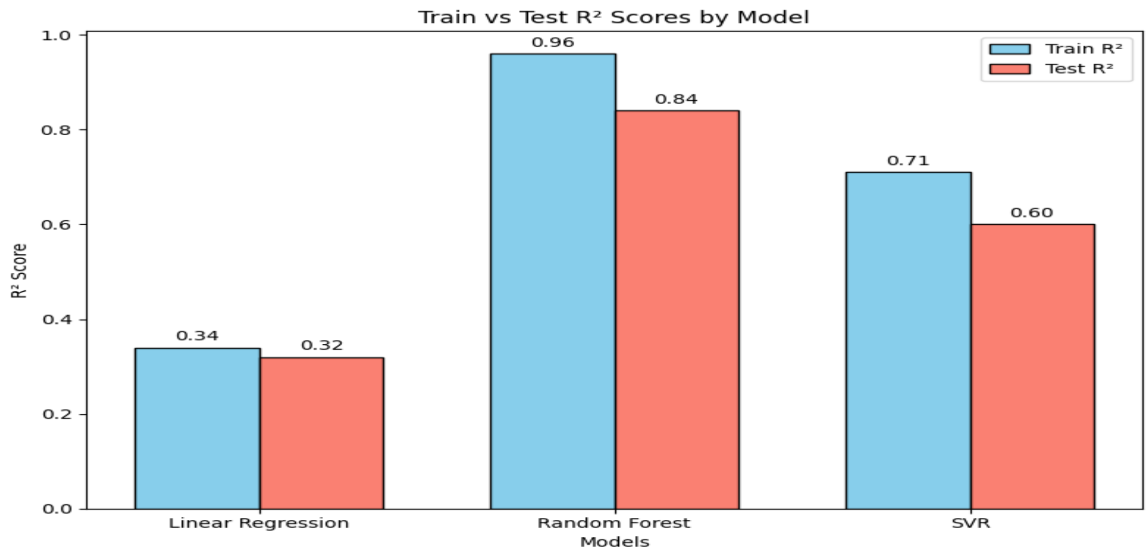

Figure 4.14**:** Train vs test R^2 of three moderated models of 100x magnification

4.4 AI MODELS TO PREDICT SR FOR 500x MAGNIFICATION DATASET

The dataset of 500x magnification contains 1320 images, split into training (953 images), validation (169 images), and testing (198 images).

4.4.1 CNN-Based Deep Learning Models For Regression for 500x Magnification Images

Images of magnification 500x have been used to train three kinds of CNN-based Deep Learning models trained to perform Regression. Image filenames were used to extract the value of surface roughness, and this value was saved to a DataFrame. The feature extraction and model training were performed after the normalization of the SEM images.

1. Simple Custom CNN Model

Training Result

The training outcome approximates the quality of the model, which is well trained to make the right predictions using the training data. The trained CNN was customized with 100 epochs and training and validation loss curves. The model was stopped in 67 epochs due to early stopping since the validation did not improve since the start of learning at 0.07365. Final training loss was 0.0999 and MAE 0.2397, and the validation loss was 0.0856 and val_MAE 0.1972.

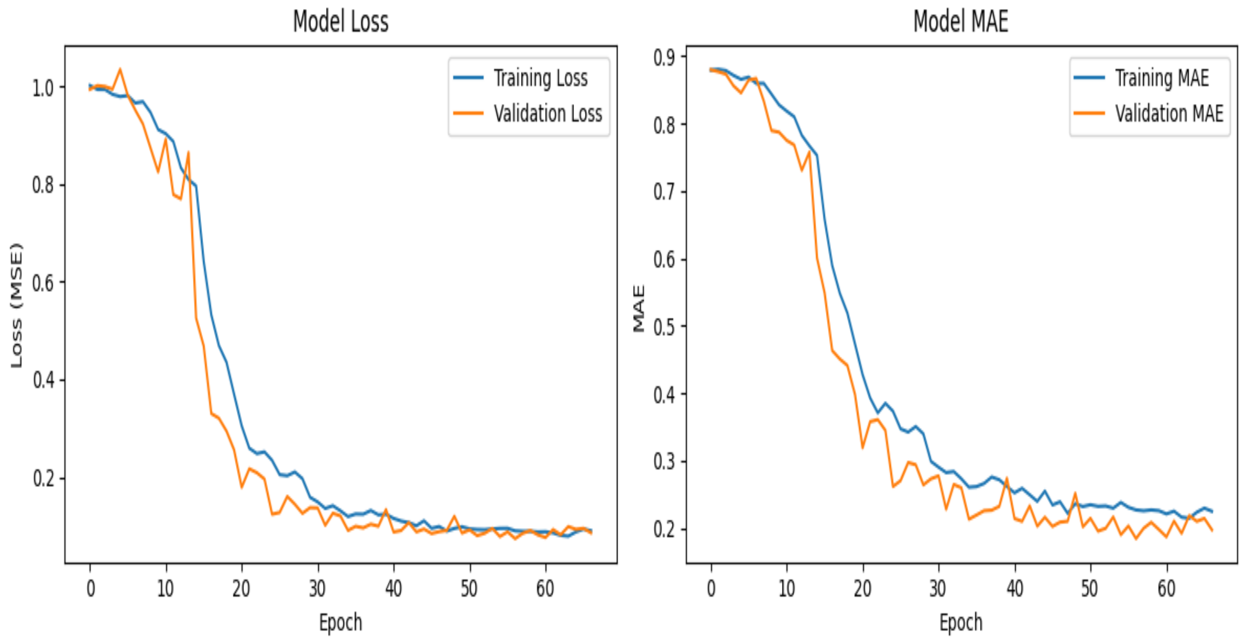

Figure 4.15: Training vs validation plots of simple CNN (500x)

The training loss monitors the model learning about the training data, while the validation loss monitors the model learning about the new and unseen data. The two measures play a crucial role in the investigation of the functioning of a machine-learning model and the avoidance of overfitting. Valid and training loss are closely related. Thus, the overfitting issue is not alarming.

Testing Result

After training the model using the training set and optimizing the loss function, the model is tested with the test set and evaluated to see the performance of the model on a previously unseen set totaling 198 images. Several evaluation metrics are normally reported against the test result, and these include MSE, RMSE, MAE, and R2. The metrics are applied to compare the performances of various models or to analyze the performance of a model in a certain task.

MSE: 0.5347

RMSE: 0.7312

MAE: 0.4631

R^2: 0.8726

The custom CNN showed an MSE of 0.5347, RMSE of 0.7312 µm, MAE of 0.4631 µm, and R^2 = 0.8726 on the test set. These statistics suggest that the model explains 87.26 percent of the variance in the roughness of surfaces, and its predictive error is, on average, 0.4631 µm

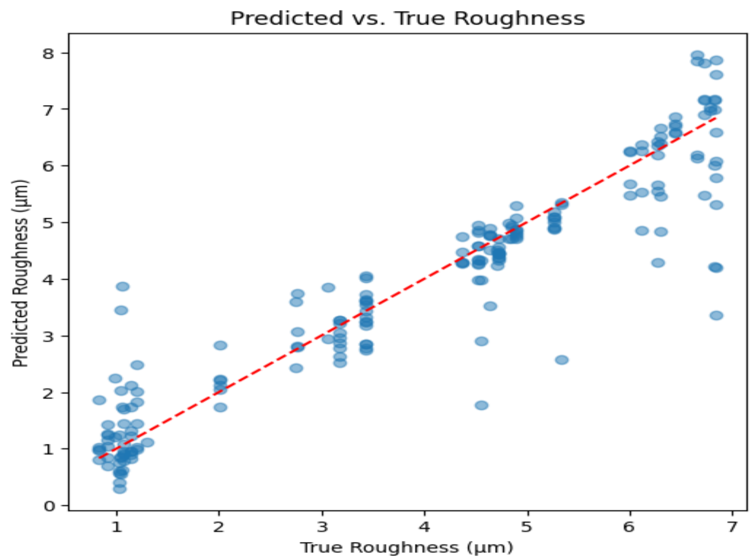

Figure 4.16: Actual vs predicted plot of simple CNN (500x)

The regression plot of the predicted and the actual roughness values indicates a strong linear relationship, with most of the predictions approximately along the dissection line, as well as the existence of minor outliers to indicate difficulty in predicting high and low roughness values.

2. ResNet50 Model

Training Result

The ResNet50 model with pretrained ImageNet weights was trained during 100 epochs, reaching the final loss values of 0.9606 and training MAE of 0.8606. As displayed in the training log, there is a gradual development, with the validation loss reading 1.0010 and validation MAE 0.8783 at epoch 12, and then stopped, as the validation did not improve from 1.0010. Thus, the result was not so good with 500x magnification in Resnet50.

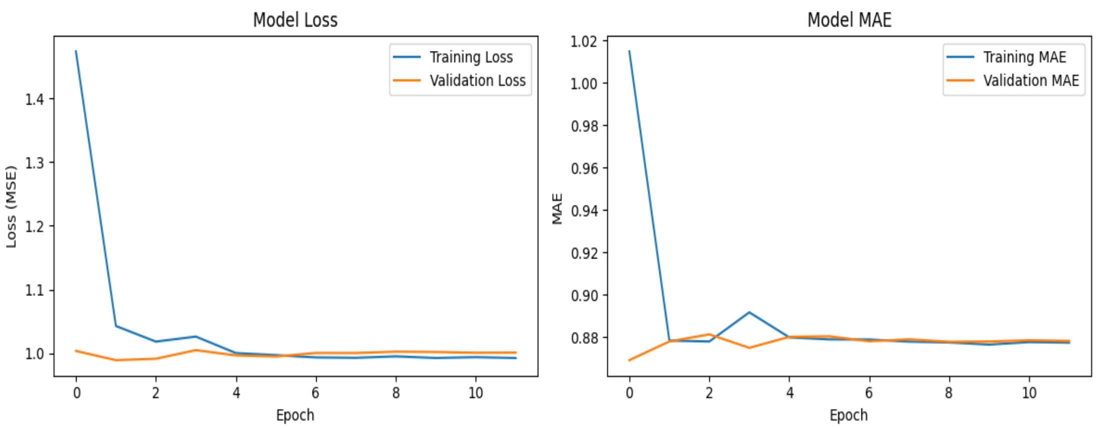

Figure 4.17: Training vs validation plots of ResNet50 (500x)

Testing Result

The results of performance metrics are-

MSE: 4.1791
RMSE: 2.0443
MAE: 1.8058
R^2: 0.1400
ResNet50 produced an MSE of 4.1791, RMSE of 2.0443 µm, MAE of 1.8058 µm, and R2 of 0.1400 on the test set. These findings reveal that the model is not so good for the magnification of 500x.

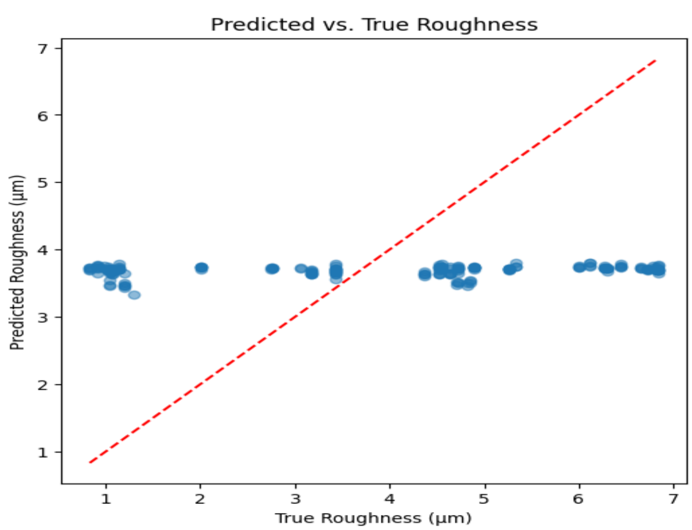

Figure 4.18: Actual vs predicted plot of ResNet50 (500x)

From the actual vs predicted graph, we can see the model is not generalizing well with the 500x magnifications, as Resnet50 was trained on RGB images, but we have used grayscale images.

3. VGG16 Model

Training Result

VGG16, which was trained on ImageNet, had an outstanding training speed, and training and validation loss curves closed quickly, at 33 epochs. Validation loss did not improve from 0.0526.

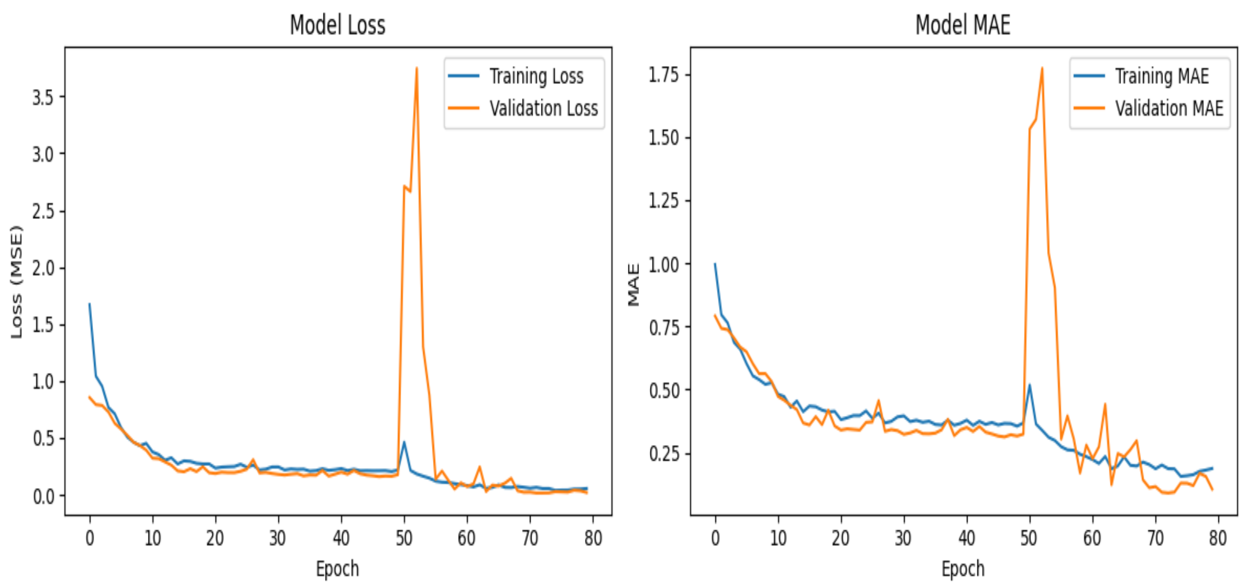

Figure 4.19: Training vs validation plots of VGG16 (500x)

From the graph, we can see the training vs validation loss and MAE. Both metrics decrease initially, indicating learning. However, there is a sharp spike in validation loss and MAE at around epoch 42, likely due to noise or imbalance. After that, both decreased again, showing that the model recovered and continued improving.

Testing Result

VGG16 was successful due to an MSE of 0.1839, RMSE of 0.4288 m, MAE of 0.2972 m, and R^2 of 0.9572 on the test set. These outcomes show that VGG16 covers 95.72 per cent of the variance in values of roughness with a small mean error of 0.2972 micrometers.

MSE: 0.1839
RMSE: 0.4288
MAE: 0.2972
R^2: 0.9502

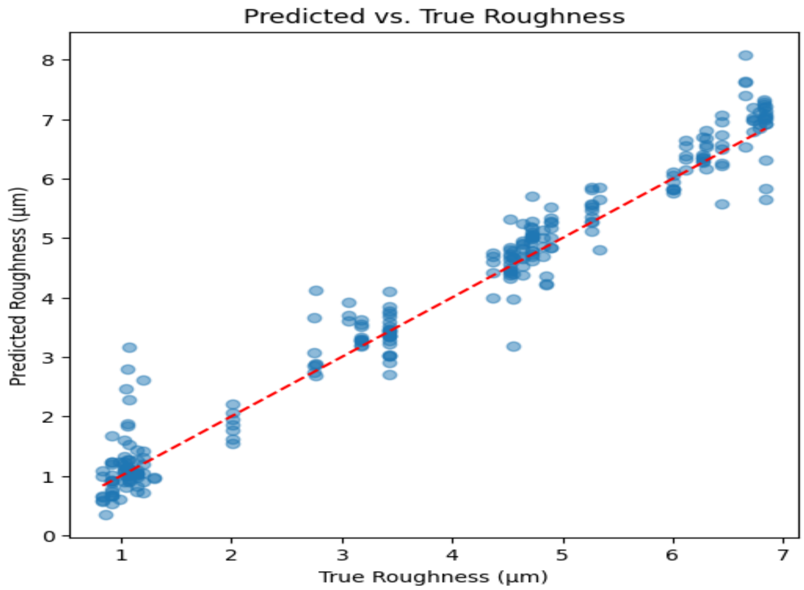

Figure 4.20: Actual vs predicted plot of VGG16 (500x)

The scatter plot indicates a close distribution of predictions around the line of equality, which once again proves the high level of accuracy and consistency of VGG16 with 500x magnification SEM images.

4.4.2 Moderated Methods using 500x Magnification Images

Images of SEM were transformed into grayscale form and binarized. Based on them, such surface features as the maximum pore area, the number of pores, the density of edges, and intensity-related features were extracted.

1. Support Vector Regression Model

To predict the roughness of a surface, the Support Vector Regression model was trained on the extracted features of SEM images at 500x magnification. The model managed to reach-

Training - MAE: 0.78, MSE: 1.25, RMSE: 1.12, R^2: 0.68

Testing - MAE: 1.02, MSE: 1.91, RMSE: 1.38, R^2: 0.55

The R^2 cross-val: 0.53

SVR used the traditional extracted features to model a nonlinear relationship through a radial basis function kernel. The value of R^2 on training data is 0.68, a test R^2 is 0.55, and the cross-validation R^2 is 0.53, illustrating a medium level of predictive power. The SVR had a lower performance than the RF, most likely due to sensitivity to a complex feature set or the hyperparameters.

2. Random Forest Regression Model

Random Forest Regression model was applied to the extracted surface features based on 500x magnification SEM images. The results are-

Training - MAE: 0.36, MSE: 0.28, RMSE: 0.53, R^2: 0.93

Testing - MAE: 0.88, MSE: 1.75, RMSE: 1.32, R^2: 0.59

Cross-Val R^2: 0.59

Using Features such as pore counts, intensity measurements, etc., which have traditionally been extracted, RF was able to model complex interactions successfully. The model fits well providing moderate generalization, training R^2= 0.93, the test-R^2= 0.59 and the cross-validation-R^2 = 0.59

3. Linear Regression Model

A Linear Regression model was developed with the results of feature extraction on SEM images at a magnification of 500x, which was used to forecast surface roughness. The training of the model and its testing were done by training, testing, and cross-validation to test its predictive values.

Training- MAE: 1.37, MSE: 2.67, RMSE: 1.63, R^2: 0.3

Testing - MAE: 1.53, MSE: 3.26, RMSE: 1.80, R^2: 0.23

Cross-val R^2: 0.28

LR is a baseline, which utilizes traditionally extracted features to describe a linear relationship. These low values of R^2 (0.31 training, 0.23 testing) show the poor ability to select the patterns, and poor generalization, which was shown to be evident in the performance on tests.

Figure 4.21: Train vs test R^2 three moderated models of 500x magnification

4.5 TESTING ON UNSEEN SEM IMAGES

The three best AI models of magnifications 150x, 100x, and 500x were applied to an unseen dataset of SEM images. The models are- simple custom CNN, VGG16, and Random Forest. Each dataset of three magnifications included 15 images for testing, and these images were never used before. The tables below show the results for the three magnifications-

Table 4.1: Prediction performance on unseen testing images across magnifications

SI	Method	Magnification	Actual Roughness	Predicted Roughness	Error (%)	Average Error(%)	Accuracy (%)	Average Accuracy(%)
1	Simple Custom CNN	150X	3.4286	3.6447	6.3024	13.49	93.6980	87.07
2			0.9058	0.8906	1.6768		98.3232	
3			3.006	2.5265	15.9519		84.0481	
4			4.8196	4.8922	1.5067		98.4933	
5			6.2772	5.7562	8.3004		91.6996	
6			1.1985	1.3824	15.3466		84.6534	
7			1.0458	1.1577	10.6972		89.3028	
8			0.853	0.4318	49.3822		50.6178	
9			4.7288	4.8002	1.5109		98.4891	
10			6.3067	6.3705	1.0116		98.9884	
11			1.0284	1.6912	65.6860		34.3130	
12			3.4227	2.9331	14.3035		85.6965	
13			2.0119	2.2589	12.2752		87.7248	
14			4.6424	4.7993	3.3794		96.6206	
15			2.7428	2.7178	0.9097		99.0903	
1			6.4377	5.9486	7.5977		92.4023	
2			2.0119	2.5356	26.0316		73.9684	
3			3.4227	3.4562	0.9782		99.0218	

4	Simple Custom CNN	100x	4.553	5.1094	12.2205	15.26	87.7795	84.73
5			6.2772	6.3008	0.3765		99.6235	
6			1.0593	1.4803	39.7413		60.2587	
7			6.7334	7.0043	4.0238		95.9762	
8			6.1157	5.8330	4.6225		95.3775	
9			3.0652	3.1691	3.3896		96.6104	
10			0.8315	1.1254	35.3483		64.6517	
11			4.728	4.7711	0.9118		99.0882	
12			2.7543	4.4637	62.0639		37.9361	
13			0.9862	1.2678	28.5515		71.4485	
14			4.7288	4.8197	1.9231		98.0769	
15			5.2655	5.2038	1.1715		98.8285	
1	Simple Custom CNN	500x	3.4286	3.5248	2.8056	18.31	97.1944	81.68
2			6.4377	6.6739	3.6692		96.3308	
3			4.5176	4.5626	0.9952		99.0048	
4			2.0119	1.8224	9.4179		90.5821	
5			3.4227	3.1726	7.3062		92.6938	
6			4.553	3.9714	12.7746		87.2254	
7			4.3732	3.4426	21.2790		78.7210	
8			1.069	2.0365	90.5095		9.4905	
9			3.0652	3.9762	29.7220		70.2780	
10			4.728	4.0209	14.9546		85.0454	
11			2.7543	3.4149	23.9839		76.0161	
12			6.2772	3.8019	39.4326		60.5674	
13			6.4377	6.6587	3.4337		96.5663	
14			2.7428	2.6034	5.0811		94.9189	
15			1.0633	0.9633	9.4030		90.5970	
1	VGG16	150X	3.4286	3.4715	1.2524	8.49	98.7476	91.5
2			0.9058	0.9470	4.5474		95.4526	
3			3.006	3.2662	8.6574		91.3426	
4			4.8196	4.7113	2.2469		97.7531	
5			6.2772	6.2274	0.7937		99.2063	
6			1.1985	1.5253	27.2640		72.7360	
7			1.0458	1.3990	33.7748		66.2252	
8			0.853	1.0225	19.8767		80.1233	
9			4.7288	4.6669	1.3082		98.6918	
10			6.3067	6.3418	0.5563		99.4437	
11			1.0284	1.1572	12.5225		87.4775	
12			3.4227	3.2352	5.4795		94.5205	
13			2.0119	1.9116	4.9865		95.0135	
14			4.6424	4.7543	2.4097		97.5903	
15			2.7428	2.7901	1.7229		98.2771	
1	VGG16	100X	6.4377	6.5432	1.6383	22.71	98.3617	77.28
2			2.0119	1.3915	30.8342		69.1658	
3			3.4227	2.1183	38.1091		61.8909	
4			4.553	3.1936	29.8568		70.1432	
5			6.2772	5.7559	8.3043		91.6957	
6			1.0593	1.6218	53.0991		46.9009	
7			6.7334	6.4770	3.8081		96.1919	
8			6.1157	4.8430	20.8109		79.1891	
9			3.0652	1.7628	42.4912		57.5088	

10			0.8315	1.3633	63.9561		36.0439	
11			4.728	3.7388	20.9218		79.0782	
12			2.7543	2.5437	7.6462		92.3538	
13			0.9862	1.0655	8.0397		91.9603	
14			4.7288	4.8935	3.4834		96.5166	
15			5.2655	5.6742	7.7609		92.2391	
1	VGG16	500x	3.4286	3.4112	0.5085	10.98	99.4915	89.01
2			6.4377	6.8622	6.5940		93.4060	
3			4.5176	4.2634	5.6271		94.3729	
4			2.0119	1.3794	31.4389		68.5611	
5			3.4227	2.5423	25.7221		74.2779	
6			4.553	4.3085	5.3690		94.6310	
7			4.3732	4.4878	2.6214		97.3786	
8			1.069	1.5375	43.8228		56.1772	
9			3.0652	3.1135	1.5765		98.4235	
10			4.728	4.8803	3.2206		96.7794	
11			2.7543	2.5646	6.8875		93.1125	
12			6.2772	5.2538	16.3034		83.6966	
13			6.4377	6.3601	1.2052		98.7948	
14			2.7428	2.6474	3.4777		96.5223	
15			1.0633	0.9521	10.4621		89.5379	
1	Random Forest	150x	3.4286	4.7060	37.2562	73.02	62.7438	26.97
2			0.9058	1.9611	116.5024		-16.5024	
3			3.006	2.4317	19.1041		80.8959	
4			4.8196	3.7039	23.1494		76.8506	
5			6.2772	5.3346	15.0170		84.9830	
6			1.1985	2.1084	75.9225		24.0775	
7			1.0458	3.9382	276.5746		-176.5746	
8			0.853	1.4544	70.5091		29.4909	
9			4.7288	3.2306	31.6814		68.3186	
10			6.3067	2.8522	54.7758		45.2242	
11			1.0284	4.1290	301.4956		-201.4956	
12			3.4227	2.7363	20.0558		79.9442	
13			2.0119	2.0928	4.0205		95.9795	
14			4.6424	4.4444	4.2653		95.7347	
15			2.7428	3.9801	45.1125		54.8875	
1	Random Forest	100x	6.4377	2.0962	67.4391	8.21	32.5609	62.71
2			2.0119	2.0998	4.3696		95.6304	
3			3.4227	1.9942	41.7354		58.2646	
4			4.553	4.4444	2.3859		97.6141	
5			6.2772	4.6862	25.3465		74.6535	
6			1.0593	1.3249	25.0755		74.9245	
7			6.7334	5.0896	24.4130		75.5870	
8			6.1157	2.0572	66.3626		33.6374	
9			3.0652	2.8506	7.0018		92.9982	
10			0.8315	1.7555	111.1260		11.1260	
11			4.728	3.0751	34.9592		65.0408	
12			2.7543	1.3552	50.7975		49.2025	
13			0.9862	1.7352	75.9450		24.0550	
14			4.7288	4.0602	14.1385		85.8615	
15			5.2655	5.6980	8.2132		91.7868	

1			3.4286	4.1605	21.3478		78.6522	
2			6.4377	3.7189	42.2319		57.7681	
3			4.5176	4.0240	10.9262		89.0738	
4			2.0119	3.8228	90.0112		9.9888	
5			3.4227	3.8672	12.9860		87.0140	
6			4.553	3.8416	15.6250		84.3750	
7			4.3732	3.9588	9.4749		90.5251	
8	Random Forest	500X	1.069	3.9543	269.9060	63.77	-169.9060	36.22
9			3.0652	3.8939	27.0362		72.9638	
10			4.728	4.0680	13.9597		86.0403	
11			2.7543	4.2032	52.6046		47.3954	
12			6.2772	3.9523	37.0375		62.9625	
13			6.4377	4.0619	36.9042		63.0958	
14			2.7428	4.2631	55.4301		44.5699	
15			1.0633	1.8993	78.3010		21.6980	

4.6 COMPARATIVE ANALYSIS

The table and figure below highlight the comparative performance of the developed models to each other at different magnifications-100x, 150x, and 500x.

Table 4.2: Comparison among the models of different magnifications

Model	Magnification	MSE	RMSE	MAE	R^2 Score
Simple CNN	150x	0.1684	0.4103	0.2763	0.9498
ResNet50	150x	0.508	1.3656	0.54	0.4696
VGG16	150x	0.0509	0.2257	0.166	0.9855
Support Vector Regression	150x	1.86	1.36	1.02	0.58
Random Forest Regression	150x	1.07	1.04	0.7	0.76
Linear Regression	150x	2.81	1.68	1.42	0.37

Simple CNN	100x	0.1738	0.4169	0.2965	0.9623
ResNet50	100x	2.8266	1.6812	1.3636	0.3504
VGG16	100x	0.1981	0.4451	0.352	0.956
Support Vector Regression	100x	1.53	1.24	0.88	0.6
Random Forest Regression	100x	0.62	0.79	0.5	0.84
Linear Regression	100x	2.56	1.6	1.21	0.32
Simple CNN	500x	0.5347	0.7312	0.4631	0.8726
ResNet50	500x	4.1791	2.0443	1.8058	0.14
VGG16	500x	0.1839	0.4288	0.2972	0.9572
Support Vector Regression	500x	1.91	1.38	1.02	0.55
Random Forest Regression	500x	1.75	1.32	0.88	0.59
Linear Regression	500x	3.26	1.8	1.53	0.23

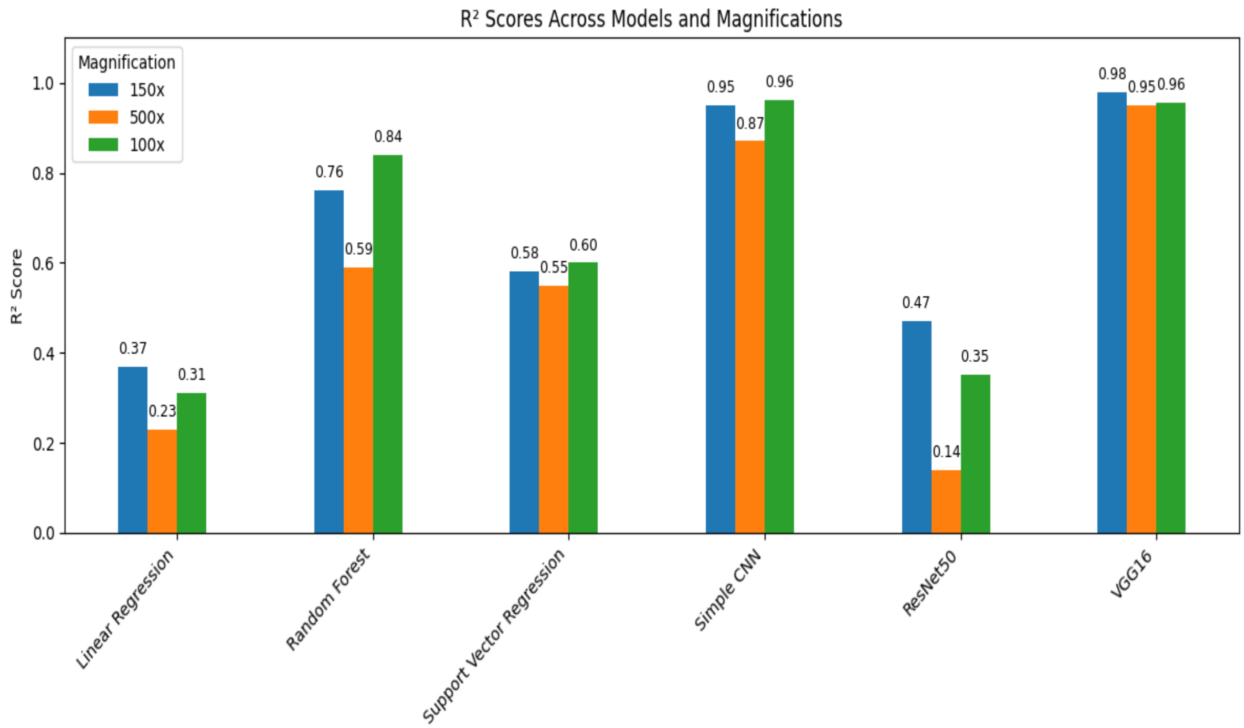

Figure 4.22: Comparison among all the models

The bar graph compares the R^2 values of the various models at three magnifications: 100x, 150x, and 500x. VGG16 was ranked best overall and had approximately 0.95-0.98 R^2 scores at all magnifications, just ahead of Simple CNN, which also performed well, in particular at 100x (0.96). Random Forest performed well, especially at 100x (0.84), although there was a considerable decline at 500x (0.59). SVR worked in a moderate range in all magnifications and had scores of about 0.55-0.60. By contrast, Linear Regression and ResNet50 performed very poorly, with ResNet50 performing significantly worse at 500x (0.14). This highlights the best use of roughness prediction of the surface using SEM images by deep learning models, especially VGG16 and CNN.

CHAPTER 5

CONCLUSIONS AND FUTURE WORK

5.1 INTRODUCTION

This chapter describes the conclusion and future research scope of this thesis work. First, the overall summary of this thesis work is presented in the conclusion section. Then, the potential future research directions are provided in the future research scope section.

5.2 CONCLUSION

In this research, a new and efficient method that uses Convolutional Neural Networks on SEM images of titanium alloy has been suggested to predict the surface roughness. Measurement methods that are used traditionally in SR tend to be limited in terms of cost, time-consuming issues during inspection, and poor adaptation to complex shapes. Comparatively, the CNN-based approaches proposed in the present study can provide an automated, non-contact solution that can scale to capture the roughness both reliably and accurately using the image data.

The custom CNN and the VGG16 models outperformed other methods in all magnifications (100x, 150x, and 500x), with VGG16 having the highest accuracy, as evidenced by R^2 scores more than 0.95. These models revealed that they had notable superiorities not only in generalization but also in prediction consistency as compared to the classic Regression, including Support Vector Regression, Random Forest, and Linear Regression. Though an experiment of ResNet50 was also carried out, this failed significantly because ResNet50 is optimized to operate with RGB images and not grayscale ones like the SEM images.

Also, this study emphasizes that the use of feature-based conventional models, in particular Random Forest, may already have a reasonable accuracy, although they fail compared to deep learning models in terms of the ability to identify complex microstructural patterns found in SEM images. Also, the findings indicate that there is a level of magnification that has some effect; models performed outstandingly at 150x and 100x, whereas at 500x, the performance was slightly lower.

This study has far-reaching implications for practice. This framework is likely to be very helpful in fields where the quality of the surface matters a lot, like aerospace, biomedical engineering, and microelectronics, as it decreases the number of manual checks needed and allows living in the world of truthful SR predictions in real-time. The study contributes to the growing body of literature on the capabilities of deep learning in materials characterization and quality control.

5.3 FUTURE WORK

An interesting development that could be taken further is to implement the trained CNN directly to the Scanning Electron Microscope itself. This integration would allow predicting the surface roughness in real-time when acquiring images, meaning that SEMs could become smart inspection devices, where early results can be immediately used to control the quality of industrial products. To go beyond theory in practice, the proposed model can be implemented and tested in real industrial settings. The practical use would require developing a user-friendly interface of the software, as well as testing it on real production lines, especially in the aerospace, biomedical devices, and microelectronics industries. Moreover, whereas this paper has focused on titanium alloys, it may look at a broader spectrum of materials that can consist of steels, ceramics, and composites. In addition, the robustness and accuracy of the models would further benefit from the addition of an extensive, diversified collection of SEM images in terms of their surface texture, magnifications, and machining parameters.

REFERENCES

[1] B. O'Neill, "Measuring surface roughness: A comprehensive guide," Wevolver, Mar. 11, 2024. [Online].Available:https://www.wevolver.com/article/measuring-surface-roughness-a-comprehensive-guide

[2] J. V. Abellán-Nebot, C. Vila Pastor, and H. R. Siller, “A Review of the Factors Influencing Surface Roughness in Machining and Their Impact on Sustainability,” Mar. 01, 2024, Multidisciplinary Digital Publishing Institute (MDPI). doi: 10.3390/su16051917.

[3] F. Rupp, L. Liang, J. Geis-Gerstorfer, L. Scheideler, and F. Hüttig, “Surface characteristics of dental implants: A review,” Jan. 01, 2018, Elsevier Inc. doi: 10.1016/j.dental.2017.09.007.

[4] M. Radmilović-Radjenović, B. Radjenović, and Z. L. J. Petrović, “Application of level set method in simulation of surface roughness in nanotechnologies,” Thin Solid Films, vol. 517, no. 14, pp. 3954–3957, May 2009, doi: 10.1016/j.tsf.2009.01.123.

[5] A. I. Sinlah, "A Study of Machinability in Milling of Austempered Ductile Iron (ADI) ADI 900, ADI 1050, and ADI 1200 with Carbide Tools," M.S. thesis, Dept. Industrial Eng., Pennsylvania State Univ., University Park, PA, 2010.

[6] N. E. Butler, "Effects of Surface Roughness and Aging on the Electrical Contact Resistance and Residual Stress in Gold-nickel-copper Connector Materials," M.S. thesis, Dept. Materials Sci. and Eng., Pennsylvania State Univ., University Park, PA, 2014.

[7] R. Russell et al., “Qualification and certification of metal additive manufactured hardware for aerospace applications,” in Additive Manufacturing for the Aerospace Industry, Elsevier, 2019, pp. 32–60. doi: 10.1016/B978-0-12-814062-8.00003-0.

[8] T. J. Webster, R. W. Siegel, and R. Bizios, “Nanoceramic surface roughness enhances osteoblast and osteoclast functions for improved orthopaedic/dental implant efficacy,” Scr Mater, vol. 44, no. 8–9, pp. 1639–1642, May 2001, doi: 10.1016/S1359-6462(01)00873-9.

[9] Bachchhav B, Bagchi H. Effect of surface roughness on friction and lubrication regimes. Materials Today: Proceedings. 2021 Jan 1;38:169-73.

[10] W. Wang, P. L. Wong, J. B. Luo, and Z. Zhang, "A new optical technique for roughness measurement on moving surface," Tribology International, vol. 31, no. 5, pp. 281–287, 1998.

[11] L. Cao, J. Li, J. Hu, H. Liu, Y. Wu, and Q. Zhou, “Optimization of surface roughness and dimensional accuracy in LPBF additive manufacturing,” Opt Laser Technol, vol. 142, p. 107246, Oct. 2021, doi: 10.1016/j.optlastec.2021.107246.

[12] F. Martín Fernández and M. J. Martín Sánchez, “Analysis of the Effect of the Surface Inclination Angle on the Roughness of Polymeric Parts Obtained with Fused Filament Fabrication Technology,” Polymers (Basel), vol. 15, no. 3, p. 585, Jan. 2023, doi: 10.3390/polym15030585.

[13] P. Mishra, S. Sood, V. Bharadwaj, A. Aggarwal, and P. Khanna, “Parametric Modeling and Opimization of Dimensional Error and Surface Roughness of Fused Deposition Modeling Printed Polyethylene Terephthalate Glycol Parts,” Polymers (Basel), vol. 15, no. 3, p. 546, Jan. 2023, doi: 10.3390/polym15030546.

[14] M. Kopp and E. Uhlmann, “Prediction of the Roughness Reduction in Centrifugal Disc Finishing of Additive Manufactured Parts Based on Discrete Element Method,” Machines, vol. 10, no. 12, p. 1151, Dec. 2022, doi: 10.3390/machines10121151.

[15] N. E. Sizemore, M. L. Nogueira, N. P. Greis, and M. A. Davies, “Application of Machine Learning to the Prediction of Surface Roughness in Diamond Machining,” Procedia Manuf, vol. 48, pp. 1029–1040, 2020, doi: 10.1016/j.promfg.2020.05.142.

[16] M. A. R. Khan, M. S. K. Asif, M. M. Rahman, and I. Ahammad, "Surface Roughness Prediction by Scanning Electron Microscope through Convolutional Neural Network," unpublished manuscript.

[17] W.-J. Lin, S.-H. Lo, H.-T. Young, and C.-L. Hung, “Evaluation of Deep Learning Neural Networks for Surface Roughness Prediction Using Vibration Signal Analysis,” Applied Sciences, vol. 9, no. 7, p. 3-17, Apr. 2019, doi: 10.3390/app9071462.

[18] M. R. Narayanan, S. Gowri, and M. M. Krishna, “On Line Surface Roughness Measurement Using Image Processing and Machine Vision,” in Proceedings of the World Congress on Engineering, London, U.K: WCE, Jul.

[19] Tribonet, "Surface roughness measurement – About Tribology," 2024. [Online]. Available: https://www.tribonet.org/wiki/surface-roughness-measurement/.

[20] P. G. Benardos and G.-C. Vosniakos, “Predicting surface roughness in machining: a review,” Int J Mach Tools Manuf, vol. 43, no. 8, pp. 833–844, Jun. 2003, doi: 10.1016/S0890-6955(03)00059-2.

[21] A. Sudianto, Z. Jamaludin, and A. Azwan Abdul Rahman, “Prediction of Surface Roughness for Development of Smart Milling Machine,” J Phys Conf Ser, vol. 1201, no. 1, p. 012008, May 2019, doi: 10.1088/1742-6596/1201/1/012008

[22] G. Samtaş, "Measurement and evaluation of surface roughness based on optic system using image processing and artificial neural network," International Journal of Advanced Manufacturing Technology, vol. 73, pp. 353–364, 2014. doi: 10.1007/s00170-014-5828-1

[23] C. Bradley, "Automated surface roughness measurement," International Journal of Advanced Manufacturing Technology, vol. 16, no. 10, pp. 668–674, 2000. doi: 10.1007/s001700070037

[24] W. Wang, P. L. Wong, J. B. Luo, and Z. Zhang, "A new optical technique for roughness measurement on moving surface," Tribology International, vol. 31, no. 5, pp. 281–287, May 1998, doi: 10.1016/s0301-679x(98)00034-6.

[25] M. Cheng et al., "Prediction of surface residual stress in end milling with Gaussian process regression,"Measurement,vol.178,p.109333,Mar.2021,doi: 10.1016/j.measurement.2021.109333.

[26] M. R. Narayanan, S. Gowri, and M. M. Krishna, "On Line Surface Roughness Measurement Using Image Processing and Machine Vision," in Proceedings of the World Congress on Engineering, London, U.K: WCE, Jul. 2007.

[27] C. Boga and T. Koroglu, "Proper estimation of surface roughness using hybrid intelligence based on artificial neural network and genetic algorithm," J Manuf Process, vol. 70, pp. 560–569, Oct. 2021, doi: 10.1016/j.jmapro.2021.08.062.

[28] N. E. Sizemore, M. L. Nogueira, N. P. Greis, and M. A. Davies, "Application of Machine Learning to the Prediction of Surface Roughness in Diamond Machining," Procedia Manuf, vol. 48, pp. 1029–1040, 2020, doi: 10.1016/j.promfg.2020.05.142.

[29] W. Zhang, "Surface Roughness Prediction with Machine Learning," Journal of Physics: Conference Series, vol. 1856, no. 1, p. 012040, Apr. 2021, doi: 10.1088/1742-6596/1856/1/012040.

[30] M. Ulas, O. Aydur, T. Gurgenc, and C. Ozel, "Surface roughness prediction of machined aluminum alloy with wire electrical discharge machining by different machine learning algorithms," Journal of Materials Research and Technology, vol. 9, no. 6, pp. 12512–12524, Nov. 2020, doi: 10.1016/j.jmrt.2020.08.098.

[31] Q. Hu, H. Xu, and Y. Chang, "Surface roughness prediction of aircraft after coating removal based on optical image and deep learning," Sci Rep, vol. 12, no. 1, p. 19407, Nov. 2022, doi: 10.1038/s41598-022-24125-5.

[32] P. M. Abhilash and A. Ahmed, "Convolutional neural network–based classification for improving the surface quality of metal additive manufactured components," The International

Journal of Advanced Manufacturing Technology, vol. 126, no. 9–10, pp. 3873–3885, Jun. 2023, doi: 10.1007/s00170-023-11388-z

[33] Md. A. R. Khan, M. M. Rahman, K. Kadirgama, M. A. Maleque, and M. Ishak, "Prediction of Surface Roughness of Ti-6Al-4V in Electrical Discharge Machining: A Regression Model," JOURNAL OF MECHANICAL ENGINEERING AND SCIENCES, vol. 1, pp. 16–18, Dec. 2011, doi: 10.15282/jmes.1.2011.2.0002.

[34] N. Chaudhary and S. A. Savari, "Simultaneous Denoising and Edge Estimation from SEM Images using Deep Convolutional Neural Networks," in 2019 30th Annual SEMI Advanced Semiconductor Manufacturing Conference (ASMC), IEEE, May 2019, pp. 1–6. doi: 10.1109/ASMC.2019.8791764.

[35] P. M. Abhilash and A. Ahmed, "Convolutional neural network–based classification for improving the surface quality of metal additive manufactured components," The International Journal of Advanced Manufacturing Technology, vol. 126, no. 9–10, pp. 3873–3885, Jun. 2023, doi: 10.1007/s00170-023-11388-z.

[36] C. He, J. Yan, S. Wang, S. Zhang, G. Chen, and C. Ren, "A theoretical and deep learning hybrid model for predicting surface roughness of diamond-turned polycrystalline materials," International Journal of Extreme Manufacturing, vol. 5, no. 3, p. 035102, Sep. 2023, doi: 10.1088/2631-7990/acdb0a.

[37] Md. A. R. Khan and M. M. Rahman, "Surface finish characteristics of titanium alloy in a non conventional technique," Materials Today Proceedings, vol. 4, no. 9, pp. 9352–9355, Jan. 2017, doi: 10.1016/j.matpr.2017.06.183.

[38] H. Sato and M. O-Hori, "Surface roughness measurement by scanning electron microscope," CIRP Annals – Manufacturing Technology, vol. 31, no. 1, pp. 457–462, 1982.

[39] Md. A. R. Khan and M. M. Rahman, "Development of regression equation for surface finish and analysis of surface integrity in EDM," World Academy of Science, Engineering and Technology, International Journal of Mechanical, Aerospace, Industrial, Mechatronic and Manufacturing Engineering, vol. 7, no. 3, pp. 464–469, Jan. 2013, [Online]. Available: http://umpir.ump.edu.my/id/eprint/6457/

[40] Md. A. R. Khan and M. M. Rahman, "Surface study in a non-conventional (Electrical discharge machining) process for Grade 6 titanium material," Jurnal Teknologi, vol. 68, no. 1, Apr. 2014, doi: 10.11113/jt.v68.1670.

[41] Md. A. R. Khan and M. M. Rahman, “Surface finish characteristics of titanium alloy in a non conventional technique,” Materials Today Proceedings, vol. 4, no. 9, pp. 9352–9355, Jan. 2017, doi: 10.1016/j.matpr.2017.06.183.

[42] Md. A. R. Khan and M. M. Rahman, “Surface characteristics of Ti-5Al-2.5Sn in electrical discharge machining using negative polarity of electrode,” The International Journal of Advanced Manufacturing Technology, vol. 92, no. 1–4, pp. 1–13, Feb. 2017, doi: 10.1007/s00170-017-0028-4.

[43] Md. A. R. Khan, M. M. Rahman, N. Zayed-Us-Salehina, and Md. S. Rahman, “Optimal set-up and surface finish characteristics in electrical discharge machining on Ti-5Al-2.5Sn using graphite,” Perspectives in Science, vol. 8, pp. 440–443, May 2016, doi: 10.1016/j.pisc.2016.04.099.

[44] Md. A. R. Khan, M. M. Rahman, and K. Kadirgama, “Neural network modeling and analysis for surface characteristics in electrical discharge machining,” Procedia Eng., vol. 90, pp. 631–636, 2014. DOI: 10.1016/j.proeng.2014.11.783.

[45] Md. A. R. Khan, M. M. Rahman, Z. Salehin, and K. Kadirgama, “Effect of discharge energy on surface finish and neural network model for surface finish,” Energy Educ. Sci. Technol. Part C: Future Energy Sources, vol. 7, no. 3, pp. 197–210, 2015.

[46] Md. A. R. Khan and M. M. Rahman, “Surface study in a non-conventional (electrical discharge machining) process for Grade 6 titanium material,” J. Teknologi (Sci. Eng.), vol. 68, no. 1, pp. 89–93, 2014. DOI: 10.11113/jt.v68.1670.

[47] Md. A. R. Khan, M. M. Rahman, and K. Kadirgama, “An experimental investigation on surface finish in die-sinking EDM of Ti-5Al-2.5Sn,” Int. J. Adv. Manuf. Technol., vol. 77, pp. 1727–1740, 2014. DOI: 10.1007/s00170-014-6507-y.

[48] Md. A. R. Khan and M. M. Rahman, “Development of regression equation for surface finish and analysis of surface integrity in EDM,” World Acad. Sci., Eng. Technol., Int. Sci. Index 75, Int. J. Mech., Ind. Sci. Eng., vol. 7, no. 3, pp. 105–110, 2013.